

~~44~~ STATION

NASA Technical Paper 1024

**COMPLETED
ORIGINAL**

Pressure and Heating-Rate Distributions on a Corrugated Surface in a Supersonic Turbulent Boundary Layer

James Wayne Sawyer

NOVEMBER 1977

NASA

84

Pressure and Heating-Rate Distributions on a Corrugated Surface in a Supersonic Turbulent Boundary Layer

James Wayne Sawyer
Langley Research Center
Hampton, Virginia



SUMMARY

An experimental investigation has been conducted to determine the drag and heating-rate penalties associated with wavy surfaces typical of current corrugated plate designs for thermal protection systems. Tests were conducted in the Langley Unitary Plan wind tunnel at Mach numbers of 2.4 and 4.5 and at unit Reynolds numbers of 3.3×10^6 per meter and 10×10^6 per meter. Both thick and thin turbulent boundary layers were obtained by respectively mounting the test plate in the tunnel wall and in a splitter plate located in the center of the tunnel stream. For each test condition, pressures and temperatures were measured with the corrugations at cross-flow angles from 0° to 90° to the flow. In addition, oil-flow patterns were obtained at a few test conditions.

Results show that for cross-flow angles of 30° or less, the pressure drag coefficients are less than the local flat-plate skin-friction coefficients and are not significantly affected by Mach number, Reynolds number, or boundary-layer thickness over the ranges investigated. For cross-flow angles greater than 30° , the drag coefficients increase significantly with cross-flow angle and increase moderately with Reynolds number. Increasing the Mach number results in a significant reduction in the pressure drag coefficients. Mach number and cross-flow angles have the most significant effect on the drag coefficients. The average and peak heating penalties due to the corrugated surface are small for cross-flow angles of 10° or less but are significantly higher for larger cross-flow angles. Mach number and Reynolds number changes have a small effect on the average heating rates, and the Reynolds number has a small effect on the peak heating rates. For the large cross-flow angles, however, the higher Mach number results in substantially higher peak heating rates. The measured heating rates correlate reasonably well with previously published results although the wave forms of the corrugations are significantly different. For small cross-flow angles, the flow remains attached to the corrugations; but for angles of 30° or greater, the flow separates from the corrugation downstream of the crest and reattaches on the upstream face of the next corrugation.

INTRODUCTION

If transportation of scientific equipment and hardware to low Earth orbit is to become economical, future space transportation systems must become fully reusable, have a long life, and have low operating cost. (See refs. 1 and 2.) Because of the extreme environment encountered by space transports, the thermal protection system plays a significant role in establishing reusability, life, and operating cost. One promising thermal protection system for such a vehicle consists of beaded or corrugated metallic panels that can maintain structural integrity under the expected high aerodynamic heating loads. (See refs. 3 and 4.) Although from a structural standpoint it is usually desirable to align the corrugations with the flow direction, local flow conditions may result in the corrugations being yawed to the mean flow direction. Consequently, the additional thermal and drag penal-

ties resulting from flow across the corrugated surface must be determined to adequately design and evaluate such metallic systems.

An experimental investigation has been conducted to determine the local heating rates and pressure distributions on a corrugated surface with a wave form typical of current metallic thermal protection systems (refs. 5 and 6). Tests were conducted in the Langley Unitary Plan wind tunnel at Mach numbers of 2.4 and 4.5 and at unit Reynolds numbers of 3.3×10^6 per meter and 10×10^6 per meter. The corrugated surface was exposed to both thick and thin turbulent boundary layers obtained by respectively mounting the test plate in the tunnel wall and in a splitter plate located in the center of the tunnel stream. For each test condition, measurements were made with the corrugations at cross-flow angles from 0° to 90° to the flow. In addition, oil-flow patterns were obtained at a few test conditions.

SYMBOLS

C_D	pressure drag coefficient
C_p	pressure coefficient, $(p_1 - p_\infty)/q_\infty$
h	heat-transfer coefficient, $\text{W/m}^2\text{-K}$
h_{av}	average heat-transfer coefficient, $\text{W/m}^2\text{-K}$
h_{fp}	flat-plate heat-transfer coefficient, $\text{W/m}^2\text{-K}$
h_{peak}	maximum heat-transfer coefficient, $\text{W/m}^2\text{-K}$
λ	wavelength of corrugations (fig. 2), cm
M_∞	free-stream Mach number
p_1	local pressure, Pa
p_∞	free-stream pressure, Pa
q_∞	free-stream dynamic pressure, Pa
R	unit Reynolds number, per meter
U	velocity, m/sec
U_∞	free-stream velocity, m/sec
x	distance measured transverse to corrugations (fig. 3), cm
y	distance measured normal to model surface, cm
δ	boundary-layer thickness, cm

δ^* boundary-layer displacement thickness, cm
 ϵ maximum wave amplitude of corrugations (fig. 2), cm
 θ momentum thickness, cm
 Λ cross-flow angle (fig. 2), deg

APPARATUS AND TESTS

Models

A photograph of the test panel mounted in the center of a large circular plate is shown in figure 1. The corrugations beside and the extensions upstream of the test plate act as fairings to minimize the edge effects. The large circular plate including the test panel and the fairings can be mounted in a splitter plate in the center of the tunnel stream to obtain a thin turbulent boundary layer over the test surface or in the tunnel wall to obtain a thick turbulent boundary layer. In either location, the circular plate can be rotated remotely during the tests to obtain flow at various cross-flow angles to the corrugations.

A detail sketch of the circular plate and test panel is shown in figure 2. The test panel is 30.48 cm by 31.85 cm and is composed of a series of circular-arc segments connected by straight-line segments as shown in view AA. The corrugations have a pitch of 8.01 cm and an amplitude that is 10 percent of the pitch. The contour of the leading-edge fairings is shown in view BB. Two models were used in the tests: one instrumented for pressure measurements and one for heat-transfer measurements. The pressure model was machined from aluminum plate and was attached to the circular plate by a strain-gage balance. A gap width of approximately 0.05 to 0.08 cm was maintained around the periphery of the test panel. The strain-gage balance attachment and the gap around the periphery of the test panel resulted from an unsuccessful attempt to measure the total drag of the test panel. The heat-transfer model was formed from a 0.05-cm-thick sheet of René 41 mounted so that the gap between the leading and ride edges of the test model and the rectangular cutout in the circular plate was nominally zero and a gap of 0.08 cm was maintained at the trailing edge to permit thermal expansion.

Instrumentation

Pressure model.—In the pressure tests, 74 pressure orifices were used. The pressure model had 62 orifices installed in the plate surface at locations shown in figure 3: 31 in each of 2 rows that extended over 2 complete wave cycles. The x-location (see view AA) of each surface orifice is listed in table I. In addition, 12 surface orifices were installed in the circular plate upstream of the test model: 6 along the crest of 1 corrugation (orifice nos. 69 to 74) and 6 along a flat (orifice nos. 63 to 68).

The orifices in both the circular plate and the test model were connected to a pressure scanning unit which allowed pressures from up to 31 orifices to be consecutively sensed by a single transducer. The transducers had a maximum range of

34.5 kPa absolute and were accurate to within ± 0.5 percent of the maximum range. Pressure measurements were taken sequentially at the rate of approximately 1 per second; thus approximately 31 seconds was required to obtain a complete pressure distribution. The pressure orifices were connected to the scanner unit by thin-wall stainless steel tubing, 0.15 cm in outside diameter.

Heat-transfer model.- The heat-transfer model had a total of 30, no. 30 gage iron-constantan thermocouples spot welded to the back side of the surface. The thermocouples were located in a straight line near the center of the plate and extended across the two center corrugations as shown in figure 4. The leads of the thermocouples were individually spot welded to the plate surface with the contact points approximately 0.3 cm apart on a line parallel to the corrugation crests. The x-location of each thermocouple is listed in table II.

Boundary-layer rake.- Boundary-layer surveys were obtained on the splitter plate with a flat surface installed. The surveys were obtained near the center of the test area using the survey rake shown by the sketch in figure 5. The rake assembly contains three total pressure probes and can be moved approximately 2.6 cm away from the splitter plate surface by remote controls. A linear potentiometer and a digital voltmeter were used to indicate the position of the rake. The bottom probe on the rake was flattened so that measurements could be made close to the wall. An internal slot width of 0.013 cm was maintained in the flattened tube.

Facility and Tests

Tests were conducted in both the low- and high-speed test sections of the Langley Unitary Plan wind tunnel at Mach numbers of 2.4 and 4.5. The low- and high-speed test sections have continuously variable Mach numbers from 1.5 to 2.86 and from 2.3 to 4.65, respectively. Further description of the wind tunnel is given in reference 7.

Pressure-distribution, heat-transfer, and oil-flow tests were conducted during this investigation. Each of the tests was conducted separately to preclude interference between measurements. A summary of the test conditions and types of tests conducted is given in table III. Tests with a thin boundary layer were conducted in the low-speed test section at a Mach number of 2.4 with the model in a splitter plate. The surface of the splitter plate was pitched at a compression angle of attack to the stream of approximately 1.5° to maintain uniform supersonic flow conditions beneath the plate. The tests with a thick boundary layer were conducted with the models mounted in the tunnel wall of the high-speed test section and at Mach numbers of 2.4 and 4.5. Test Reynolds numbers of 3.3×10^6 per meter and 10×10^6 per meter were obtained in each test section. Heating-rate measurements were obtained only for the model mounted in the tunnel wall and thus under a thick boundary layer. Boundary-layer surveys were made only on the splitter plate since wall boundary-layer surveys had been made previously.

For the pressure-distribution and oil-flow tests, measurements were taken soon after test conditions were established. For the heat-transfer tests, the test sequence was as follows. The tunnel was started and run for approximately 1 hour to stabilize the temperature of the tunnel walls and the stream. Then the

flow was diverted through a cooler which rapidly reduced the total temperature of the stream and the temperature of the thin model surface. The flow was then rediverted and the total temperature of the stream increased rapidly to give a heat pulse. The heat pulse typically consisted of a rise in total temperature of approximately 65 K in 8 seconds, as indicated in figure 6 where typical total and surface temperatures are shown. Temperature measurements were recorded every 0.5 second for 45 seconds after the beginning of the heat pulse.

Heat-Transfer Data Reduction

Heat-transfer coefficients were obtained from transient skin temperatures resulting from a step-wise increase in the stagnation temperature as discussed previously. Calculations were made when the total temperature first became stable. The data were reduced to coefficient form by assuming constant temperature through the skin thickness and accounting for lateral heat flow transverse to the corrugations. The heat flow to the model interior, the heat loss due to radiation, and the lateral heat flow parallel to the corrugations were neglected. A more detailed discussion of the heat-transfer data reduction technique is given in reference 7.

RESULTS AND DISCUSSION

Typical boundary-layer velocity distributions obtained on a flat surface in both the splitter plate and the tunnel wall are shown in figure 7. The data on the splitter plate at $M_{\infty} = 2.4$ were obtained during the present investigation. The data on the tunnel wall at $M_{\infty} = 2.86$ were obtained during an unpublished investigation similar to that reported in reference 8. The boundary-layer thickness (based on U/U_{∞} of approximately 0.99) on the splitter plate and on the wall was approximately 2.5 cm and 12.7 cm, respectively. Neither Reynolds number nor Mach number changes for the range of this investigation significantly altered the boundary-layer thickness or velocity distribution.

During this investigation, a considerable quantity of data was obtained. However, only a limited number of the pressure and heating-rate distributions are plotted to show typical trends and flow phenomena; a complete listing of the pressure and heat-transfer coefficients is given in tables IV to VII. In tables IV to VI, pressure coefficients C_p are given for each pressure orifice for flow at various cross-flow angles Λ to the corrugations: table IV is for $M_{\infty} = 2.4$ and $\delta = 2.5$ cm, table V is for $M_{\infty} = 2.4$ and $\delta = 12.7$ cm, and table VI is for $M_{\infty} = 4.5$ and $\delta = 12.7$ cm. In table VII, heat-transfer coefficients h are given at each thermocouple location for flow at various angles to the corrugations.

Pressure Distributions

Pressure measurements were made over two corrugation wavelengths at two locations on the test panel. (See fig. 3.) Pressure coefficients from the two locations differ by up to 80 percent for the thin boundary layer and $\Lambda = 45^\circ$. Flow distortions due to the transition upstream of the test panel from a flat plate to a corrugated surface probably caused these differences in pressure. Since the downstream row of orifices is farthest from the leading edge, flow distortions

should have a minimum effect at that location; thus, the pressure coefficients measured at the downstream location (orifice nos. 32 to 62) are used for further discussion.

Effects of boundary-layer thickness.— The effects of boundary-layer thickness on the pressure distributions are shown in figure 8 for $M_{\infty} = 2.4$ and $R = 10 \times 10^6$ per meter. Pressure distributions are presented for a thin ($\delta = 2.5$ cm) and a thick ($\delta = 12.7$ cm) turbulent boundary layer and for flow at 0° , 15° , 30° , and 45° to the corrugations. The C_p values shown for the 2.5-cm boundary layer have been adjusted to account for the 1.5° angle of attack at which the measurements were made. The good agreement of the data shows that the boundary-layer thickness has only a small effect on the C_p distributions.

For $\Lambda = 0^\circ$ (fig. 8(a)), the C_p values are approximately zero. For $\Lambda > 0^\circ$ (figs. 8(b), 8(c), and 8(d)), variations in C_p were obtained which are slightly out of phase with the corrugations. The maximum values occur upstream of the corrugation crests and the minimum values occur on the downstream side of the corrugation crests. Further, the C_p values increase in magnitude as Λ increases to 45° . For $\Lambda = 30^\circ$ and 45° , the C_p values are nearly constant on a portion of the downstream side of the corrugations and on the flats. This plateau in the C_p distribution suggests the possibility of flow separation which is discussed subsequently.

Effects of Reynolds number.— The effects of Reynolds number on the pressure distributions are shown in figure 9 for four cross-flow angles with $\delta = 12.7$ cm and $M_{\infty} = 2.4$. Data are shown for $R = 3.3 \times 10^6$ per meter and for $R = 10 \times 10^6$ per meter. This variation in Reynolds number had little effect on the pressure distributions or the location where the maximum and minimum pressure coefficients occur. This result agrees with other experimental and theoretical investigations published in the literature. (See, for example, refs. 9 and 10.)

Effects of Mach number.— Pressure distributions obtained at Mach numbers of 2.4 and 4.5 are compared in figure 10 for $\delta = 12.7$ cm and $R = 10 \times 10^6$ per meter. As shown in the figure, Mach number does not significantly change the basic shape of the pressure-distribution curves although the locations of the maximum and minimum pressure coefficients shift slightly. However, for $\Lambda > 0^\circ$, Mach number has a significant effect on the magnitude of the pressure coefficients. Increasing M_{∞} from 2.4 to 4.5 reduces the pressure coefficients by more than 50 percent. The large reduction in C_p with increasing Mach number agrees with results presented in references 11 and 12 for corrugations with similar ratios of amplitude to pitch. The lower pressure coefficients obtained at the higher Mach number suggest that the pressure drag coefficients may also be significantly lower.

Pressure Drag

Drag coefficients C_D obtained by integrating the pressure coefficients over the corrugated surface are presented as a function of cross-flow angle in figures 11(a) and 11(b) for thin and thick turbulent boundary layers, respectively. Data are given for $M_{\infty} = 2.4$ at $R = 3.3 \times 10^6$ per meter and for

$M_\infty = 2.4$ and 4.5 at $R = 10 \times 10^6$ per meter. For $\Lambda \leq 30^\circ$, the pressure drag coefficients are less than the local flat-plate skin-friction coefficients given by reference 13 and are not significantly affected by variations in Mach number, Reynolds number, or boundary-layer thickness. For $\Lambda \geq 45^\circ$, the drag coefficients are significantly higher than the flat-plate skin-friction drag. For $M_\infty = 2.4$, increasing R results in an increase in C_D , although the effect is more pronounced in the thin boundary layer. (Compare figs. 11(a) with 11(b).) For $R = 10 \times 10^6$ per meter and $\delta = 12.7$ cm (fig. 11(b)), decreasing the Mach number from 4.5 to 2.4 shows a pronounced increase in C_D . At $\Lambda = 90^\circ$, the C_D at $M_\infty = 2.4$ is more than double that at $M_\infty = 4.5$.

Heating-Rate Distributions

Typical heating-rate distributions are shown in figure 12 where the normalized heat-transfer coefficients h/h_{fp} are shown across two corrugations under a thick ($\delta = 12.7$ cm) turbulent boundary layer (no heating-rate measurements were made with the thin boundary layer). Distributions are presented for flow at 0° , 15° , 30° , and 45° to the corrugations. Curves are presented for $M_\infty = 2.4$ and $R = 3.3 \times 10^6$ per meter, for $M_\infty = 2.4$ and $R = 10 \times 10^6$ per meter, and for $M_\infty = 4.5$ and $R = 10 \times 10^6$ per meter. The heat-transfer coefficients are normalized by the flat-plate heat-transfer coefficients h_{fp} interpolated from the data presented in references 7 and 8. For $\Lambda = 0^\circ$ (fig. 12(a)), the heating-rate distributions are in phase with the corrugated surface: the maximum h/h_{fp} values occur on the crests and the minimum values occur on the flats. For $\Lambda > 0^\circ$ (figs. 12(b), 12(c), and 12(d)), the heating-rate distributions shift upstream: the maximum h/h_{fp} values occur upstream of the corrugation crests and the minimum values occur on the downstream side of the corrugations. For $\Lambda \geq 15^\circ$ (e.g., fig. 12(b)), the h/h_{fp} values increase even across the flats. For $\Lambda = 30^\circ$ (fig. 12(c)) and $\Lambda = 45^\circ$ (fig. 12(d)), relatively low heating rates are obtained in the region downstream of the corrugation crest. The low heating region coincides approximately with the constant-pressure region noted in figure 8 and is thought to result from flow separation.

Average and Peak Heating

Average and peak heating rates for the corrugated surface under a thick ($\delta = 12.7$ cm) turbulent boundary layer are presented as a function of cross-flow angle in figure 13. The heat-transfer coefficients have been normalized by flat-plate values interpolated from data presented in references 7 and 8. The average heating rates were obtained by integrating the experimental heat-transfer coefficients over the surface of the corrugations. Data are given at $R = 3.3 \times 10^6$ per meter for $M_\infty = 2.4$ and at $R = 10 \times 10^6$ per meter for $M_\infty = 2.4$ and 4.5 . The average heating rates shown in figure 13(a) are relatively small for $0^\circ < \Lambda < 10^\circ$. For $\Lambda > 10^\circ$, the average heating rate increases significantly with an increase in Λ . Mach number and Reynolds number changes do not have a significant effect on the average heating rates. For $\Lambda = 45^\circ$, the average heating rate is approximately 40 percent higher than the flat-plate value.

The peak heating rates shown in figure 13(b) are also small and approximately constant for $0^\circ < \Lambda < 10^\circ$, and they increase significantly with Λ for $\Lambda > 10^\circ$.

For $M_{\infty} = 2.4$ and $\Lambda \geq 30^\circ$, increasing the Reynolds number results in a slight decrease in the peak heating. For the high Reynolds number, increasing the Mach number from 2.4 to 4.5 significantly increases the peak heating. For $\Lambda = 45^\circ$, the peak heating rate is 80 to 140 percent higher than the flat-plate values.

The peak heating data obtained in the present investigation are compared in figure 14 with data published in references 7, 9, 11, 12, 14, and 15. The parameter used to correlate the data was developed in reference 9. It is

$$1 + \frac{1}{e^{6.614}} \sin \Lambda \frac{M_{\infty}^{1.097}}{(\epsilon/l)^{0.526}} R^{0.42} \left(\frac{\delta^*}{l} \right)^{0.148} \frac{1}{(\theta/l)^{0.208}}$$

It should be pointed out that the corrugations used in these references have wave forms significantly different from that of the present investigation. In figure 14, the data from the present investigation and the references are shown by the test-point symbols, and the solid line indicates perfect correlation. The present data are in reasonable agreement with the previously published results but are above the correlation curve. For the present data with a high Reynolds number, variations in the cross-flow angle generally result in variations in peak heating values that parallel the correlation curve. The low Reynolds number and low Mach number data, although consistent within themselves, have a steeper slope than the correlation curve. No attempt was made in this investigation to improve the correlation expression.

Oil-Flow Studies

The possibility of flow separation for certain cross-flow angles was investigated by obtaining oil-flow patterns. Typical flow patterns over the corrugated surface for $M_{\infty} = 2.4$, $R = 10 \times 10^6$ per meter, and $\delta = 12.7$ cm are shown in figure 15 for cross-flow angles of 0° , 15° , 30° , and 45° . For $\Lambda = 30^\circ$ and 45° , flow separation appears to occur on the downstream side of the corrugations at the locations shown on the figure. This result agrees with the variations in the pressure and heating rate distributions noted previously. Reattachment appears to occur on the windward side of the corrugations, approximately where the peak pressure coefficients occurred in figure 8. Flow separation is not evident for cross-flow angles of 0° and 15° .

CONCLUDING REMARKS

An experimental investigation was conducted to determine the drag and heating-rate penalties on wavy surfaces typical of current corrugated plate designs for thermal protection systems. Tests were conducted in the Langley Unitary Plan wind tunnel at Mach numbers of 2.4 and 4.5 and at unit Reynolds numbers of 3.3×10^6 per meter and 10×10^6 per meter. The corrugated surface was exposed to both thick and thin turbulent boundary layers obtained by respectively mounting the test plate in the tunnel wall and in a splitter plate located in the center of the tunnel stream. For each test condition, measurements were made with the corrugations at cross-flow

angles from 0° to 90° to the flow. In addition, oil-flow patterns were obtained at a few test conditions.

Results show that for cross-flow angles of 30° or less, the pressure drag coefficients are less than the local flat-plate skin-friction coefficients and are not significantly affected by Mach number, Reynolds number, or boundary-layer thickness over the ranges investigated. For cross-flow angles greater than 30° , the drag coefficients increase significantly with cross-flow angle and moderately with Reynolds number. Increasing Mach number causes significant reductions in the pressure drag coefficients. The average and peak heating penalties due to the corrugated surface are small for cross-flow angles of 10° or less but are significantly higher for the larger cross-flow angles. Mach number and Reynolds number changes have a small effect on the average heating rates, and the Reynolds number has small effect on the peak heating rates. However, for the large cross-flow angles, the higher Mach number results in substantially higher peak heating rates. The measured peak heating rates correlate reasonably well with previously published results even though the wave forms of the corrugations are significantly different. For small cross-flow angles, the flow remains attached to the corrugations, but for angles of 30° or greater, the flow separates from the corrugation downstream of the crest and reattaches on the upstream face of the next corrugation.

Langley Research Center
National Aeronautics and Space Administration
Hampton, VA 23665
August 25, 1977

REFERENCES

1. Outlook for Space. Report to the NASA Administrator by the Outlook for Space Study Group. NASA SP-386, 1976.
2. Henry, Beverly Z.; and Decker, John P.: Future Earth Orbit Transportation Systems/Technology Implications. *Astronaut. & Aeronaut.*, vol. 14, no. 9, Sept. 1976, pp. 18-28.
3. Stein, Bland A.; Bohon, Herman L.; and Rummel, Donald R.: An Assessment of Radiative Metallic Thermal Protection Systems for Space Shuttle. *NASA Space Shuttle Technology Conference - Dynamics and Aeroelasticity; Structures and Materials*, NASA TM X-2570, 1972, pp. 267-302.
4. Bohon, Herman L.; Shideler, John L.; and Rummel, Donald R.: Radiative Metallic Thermal Protection Systems - A Status Report. *NASA paper presented at 18th Structures, Structural Dynamics and Materials (San Diego, California) Conference*, Mar. 1977.
5. Deveikis, William D.; Miserentino, Robert; Weinstein, Irving; and Shideler, John L.: Aerothermal Performance and Structural Integrity of a René 41 Thermal Protection System at Mach 6.6. *NASA TN D-7943*, 1975.
6. Sawyer, James Wayne: Aerothermal and Structural Performance of a Cobalt-Base Superalloy Thermal Protection System at Mach 6.6. *NASA TN D-8415*, 1977.
7. Stallings, Robert L., Jr.; and Collins, Ida K.: Heat-Transfer Measurements on a Flat Plate and Attached Protuberances in a Turbulent Boundary Layer at Mach Number of 2.65, 3.51, and 4.44. *NASA TN D-2428*, 1964.
8. Burbank, Paige B.; Newlander, Robert A.; and Collins, Ida K.: Heat-Transfer and Pressure Measurements on a Flat-Plate Surface and Heat-Transfer Measurements on Attached Protuberances in a Supersonic Turbulent Boundary Layer at Mach Numbers of 2.65, 3.51, and 4.44. *NASA TN D-1372*, 1962.
9. Brandon, H. J.; and Masek, R. V.: Measurement and Correlation of Aerodynamic Heating to Surface Corrugation Stiffened Structures in Thick Turbulent Boundary Layers. *NASA CR-132503*, [1974].
10. Polak, A.; Werle, M. J.; Yatsa, V. N.; and Bertke, S. D.: Numerical Study of Separated Laminar Boundary Layers Over Multiple Sine-Wave Protuberances. *J. Spacecr. & Rockets*, vol. 13, no. 3, Mar. 1976, pp. 168-173.
11. Cary, Aubrey M., Jr.; and Morrisette, E. Leon: Effect of Two-Dimensional Multiple Sine-Wave Protrusions on the Pressure and Heat-Transfer Distributions for a Flat Plate at Mach 6. *NASA TN D-4437*, 1968.
12. Weinstein, Leona d M.: Effects of Two-Dimensional Sinusoidal Waves on Heat Transfer and Pressure Over a Flat Plate at Mach 8.0. *NASA TN D-5937*, 1970.
13. Schlichting, Hermann (J. Kestin, transl.): *Boundary Layer Theory*. Fourth ed. McGraw-Hill Book Co., Inc., c.1960.

14. Shore, Charles P.; Dixon, Sidney C.; and Griffith, George E.: Experimental Pressure and Turbulent Heat-Transfer Coefficients Associated With Sinusoidal Protuberances on a Flat Plate at a Mach Number of 3. NASA TN D-1626, 1963.
15. Jaeck, C. L. (appendix A by R. T. Savage and A. L. Nagel): Analysis of Pressure and Heat Transfer Tests on Surface Roughness Elements With Laminar and Turbulent Boundary Layers. NASA CR-537, 1966.

TABLE I.- PRESSURE ORIFICE LOCATION

Orifice no.	x*, cm
1	0
2	.52
3	1.03
4	1.53
5	2.02
6	2.50
7	3.08
8	3.69
9	4.30
10	4.91
11	5.48
12	5.99
13	6.48
14	6.98
15	7.50
16	8.01
17	8.53
18	9.04
19	9.54
20	10.04
21	10.51
22	11.09
23	11.70
24	12.31
25	12.92
26	13.52
27	14.00
28	14.49
29	14.99
30	15.51
31	16.02

*See figure 3.

TABLE II.- THERMOCOUPLE LOCATIONS

Thermocouple no.	x*, cm	Thermocouple no.	x*, cm
1	0.31	16	8.32
2	.92	17	8.93
3	1.49	18	9.53
4	2.00	19	10.01
5	2.49	20	10.50
6	2.99	21	11.00
7	3.51	22	11.52
8	4.02	23	12.03
9	4.54	24	12.55
10	5.05	25	13.06
11	5.55	26	13.56
12	6.05	27	14.05
13	6.52	28	14.53
14	7.10	29	15.11
15	7.71	30	15.72

*See figure 4.

TABLE III.- TEST CONDITIONS AND MEASUREMENTS

δ , cm	M_∞	R, per meter	q_∞ , kPa	Measurements			
				Pressure	Heating rate	Boundary-layer survey	Oil-flow patterns
2.5	2.4	3.3×10^6	10.6	✓		✓	✓
		10	32.0	✓		✓	
12.7	2.4	3.3×10^6	10.6	✓	✓		
		10	32.0	✓	✓		✓
	4.5	10×10^6	17.6	✓	✓		

TABLE IV.- PRESSURE COEFFICIENT DATA AT $M_{\infty} = 2.4$ AND $\delta = 2.5$ cm(a) $\Lambda = 0^\circ$

Orifice no.	C _p at -		Orifice no.	C _p at -		Orifice no.	C _p at -	
	R = 3.3 × 10 ⁶ per m	R = 10 × 10 ⁶ per m		R = 3.3 × 10 ⁶ per m	R = 10 × 10 ⁶ per m		R = 3.3 × 10 ⁶ per m	R = 10 × 10 ⁶ per m
1	0.0304	0.0236	32	0.0333	0.0232	63	0.0444	0.0314
2	.0297	.0236	33	.0333	.0242	64	.1285	.1197
3	.0308	.0250	34	.0343	.0251	65	.1051	.0987
4	.0327	.0266	35	.0354	.0258	66	.0556	.0504
5	.0337	.0288	36	-----	-----	67	.0323	.0260
6	.0351	.0305	37	-----	-----	68	.0233	.0106
7	.0361	.0318	38	-----	-----	69	.1529	.1459
8	.0362	.0317	39	-----	-----	70	.0935	.0853
9	.0360	.0320	40	.0365	.0267	71	.0402	.0282
10	.0357	.0317	41	.0378	.0265	72	.0312	.0190
11	.0344	.0303	42	.0393	.0265	73	.0504	.0425
12	.0333	.0290	43	.0771	.0348	74	.0479	.0425
13	.0319	.0279	44	.0459	.0270			
14	.0296	.0248	45	.0474	.0263			
15	.0284	.0239	46	.0482	.0262			
16	.0249	.0237	47	.0477	.0246			
17	.0300	.0234	48	.0467	.0239			
18	.0322	.0266	49	.0432	.0236			
19	.0338	.0278	50	.0391	.0227			
20	.0365	.0315	51	.0358	.0218			
21	.0385	.0338	52	.0328	.0216			
22	.0409	.0374	53	.0312	.0224			
23	.0404	.0362	54	.0274	.0198			
24	.0408	.0355	55	.0256	.0201			
25	.0406	.0355	56	.0259	.0213			
26	.0409	.0345	57	.0249	.0199			
27	.0384	.0334	58	.0242	.0202			
28	.0369	.0312	59	.0233	.0181			
29	.0324	.0289	60	.0229	.0184			
30	.0297	.0259	61	-----	-----			
31	.0276	.0252	62	.0222	.0165			

TABLE IV.- Continued

(b) $A = 59$

Orifice no.	C _p at -		Orifice no.	C _p at -		Orifice no.	C _p at -	
	R = 3.3 × 10 ⁶ per sec	R = 10 × 10 ⁶ per sec		R = 3.3 × 10 ⁶ per sec	R = 10 × 10 ⁶ per sec		R = 3.3 × 10 ⁶ per sec	R = 10 × 10 ⁶ per sec
1	0.0335	0.0276	32	0.0320	0.0220	63	0.0424	0.0319
2	.0304	.0242	33	.0312	.0219	64	.1228	.1162
3	.0287	.0224	34	.0316	.0217	65	.1027	.0990
4	.0288	.0226	35	.0321	.0223	66	.0560	.0519
5	.0284	.0227	36	-----	-----	67	.0362	.03
6	.0303	.0243	37	-----	-----	68	.0287	.0183
7	.0337	.0270	38	-----	-----	69	.1503	.1482
8	.0344	.0286	39	-----	-----	70	.0925	.0875
9	.0362	.0310	40	.0352	.0246	71	.0404	.0307
10	.0377	.0323	41	.0370	.0259	72	.0235	.0130
11	.0380	.0337	42	.0385	.0256	73	.0402	.0320
12	.0387	.0342	43	.0756	.0349	74	.0420	.0363
13	.0383	.0347	44	.0448	.0265			
14	.0363	.0322	45	.0466	.0261			
15	.0345	.0304	46	.0477	.0265			
16	.0327	.0286	47	.0475	.0263			
17	.0297	.0248	48	.0455	.0252			
18	.0295	.0245	49	.0424	.0249			
19	.0297	.0237	50	.0389	.0247			
20	.0308	.0252	51	.0351	.0236			
21	.0327	.0281	52	.0329	.0240			
22	.0367	.0332	53	.0317	.0245			
23	.0374	.0335	54	.0278	.0224			
24	.0387	.0334	55	.0265	.0212			
25	.0409	.0359	56	.0271	.0229			
26	.0434	.0381	57	.0242	.0197			
27	.0425	.0382	58	.0206	.0170			
28	.0428	.0379	59	.0177	.0138			
29	.0391	.0367	60	.0160	.0130			
30	.0355	.0328	61	-----	-----			
31	.0317	.0309	62	.0141	.0108			

TABLE IV.- Continued

(c) $\Delta = 100$

Orifice no.	C _p at -		Orifice no.	C _p at -		Orifice no.	C _p at -	
	R = 3.3 × 10 ⁶ per m	R = 10 × 10 ⁶ per m		R = 3.3 × 10 ⁶ per m	R = 10 × 10 ⁶ per m		R = 3.3 × 10 ⁶ per m	R = 10 × 10 ⁶ per m
1	0.0338	0.0287	32	0.0294	0.0179	63	0.0448	0.0339
2	.0326	.0282	33	.0304	.0194	64	.1166	.1090
3	.0318	.0279	34	.0326	.0214	65	.1054	.0937
4	.0324	.0286	35	.0351	.0247	66	.0640	.0581
5	.0335	.0292	36	-----	-----	67	.0501	.0453
6	.0347	.0302	37	-----	-----	68	.0435	.0356
7	.0358	.0314	38	-----	-----	69	.1521	.1491
8	.0373	.0324	39	-----	-----	70	.0948	.0860
9	.0386	.0327	40	.0416	.0304	71	.0420	.0322
10	.0404	.0339	41	.0436	.0213	72	.0124	.0026
11	.0386	.0314	42	.0447	.0304	73	.0.53	.0015
12	.0365	.0285	43	.0797	.0376	74	.0255	.0149
13	.0354	.0279	44	.0451	.0239			
14	.0340	.0270	45	.0432	.0203			
15	.0343	.0276	46	.0430	.0186			
16	.0344	.0296	47	.0433	.0183			
17	.0336	.0284	48	.0435	.0193			
18	.0338	.0301	49	.0431	.0227			
19	.0341	.0303	50	.0420	.0256			
20	.0348	.0312	51	.0405	.0270			
21	.0365	.0319	52	.0397	.0286			
22	.0387	.0350	53	.0389	.0307			
23	.0394	.0352	54	.0365	.0299			
24	.0395	.0336	55	.0355	.0307			
25	.04.2	.0348	56	.0363	.0323			
26	.0414	.0334	57	.0346	.0304			
27	.0378	.0302	58	.0296	.0251			
28	.0370	.0287	59	.0228	.0174			
29	.0340	.0289	60	.0164	.0120			
30	.0332	.0284	61	-----	-----			
31	.0323	.0297	62	.0085	.0024			

TABLE IV.- Continued

(d) $\Delta = 15^\circ$

Orifice no.	C _p at -		Orifice no.	C _p at -		Orifice no.	C _p at -	
	R = 3.3 × 10 ⁶ per m	R = 10 × 10 ⁶ per m		R = 3.3 × 10 ⁶ per m	R = 10 × 10 ⁶ per m		R = 3.3 × 10 ⁶ per m	R = 10 × 10 ⁶ per m
1	0.0156	0.0059	32	0.0182	0.0075	63	0.0456	0.0376
2	.0224	.0163	33	.0189	.0078	64	.1048	.0986
3	.0285	.0257	34	.0244	.0139	65	.1054	.1019
4	.0338	.0325	35	.0323	.0230	66	.0734	.0687
5	.0376	.0364	36	-----	-----	67	.0654	.0628
6	.0391	.0375	37	-----	-----	68	.0591	.0537
7	.0389	.0377	38	-----	-----	69	.1498	.1465
8	.0462	.0460	39	-----	-----	70	.0941	.0872
9	.0520	.0500	40	.0456	.0334	71	.0371	.0296
10	.0544	.0519	41	.0464	.0351	72	-.0013	-.0070
11	.0465	.0432	42	.0506	.0395	73	-.0104	-.0199
12	.0346	.0285	43	.0855	.0480	74	-.0045	-.0231
13	.0243	.0164	44	.0495	.0318			
14	.0159	.0040	45	.0441	.0218			
15	.0137	.0025	46	.0384	.0151			
16	.0174	.0106	47	.0341	.0091			
17	.0242	.0196	48	.0318	.0087			
18	.0314	.0299	49	.0336	.0147			
19	.0365	.0357	50	.0369	.0226			
20	.0402	.0397	51	.096	.0277			
21	.0418	.0405	52	.0407	.0311			
22	.0423	.0413	53	.0410	.0331			
23	.0483	.0490	54	.0397	.0314			
24	.0526	.0524	55	.0387	.0298			
25	.0555	.0521	56	.0387	.0319			
26	.0494	.0452	57	.0376	.0336			
27	.0361	.0296	58	.0337	.0310			
28	.0234	.0156	59	.0254	.0217			
29	.0098	.0026	60	.0166	.0122			
30	.0059	-.0017	61	-----	-----			
31	.0081	.0040	62	.0043	-.0016			

15

TABLE IV.- Continued

(e) $\Delta = 20^\circ$

Orifice no.	C_p at -		Orifice no.	C_p at -		Orifice no.	C_p at -	
	$R = 3.3 \times 10^6$ per m	$R = 10 \times 10^6$ per m		$R = 3.3 \times 10^6$ per m	$R = 10 \times 10^6$ per m		$R = 3.3 \times 10^6$ per m	$R = 10 \times 10^6$ per m
1	-0.0076	-0.0323	32	0.0151	0.0031	63	0.0512	0.0426
2	.0059	-.0041	33	.0165	.0079	64	.0969	.0880
3	.0225	.0210	34	.0248	.0195	65	.1127	.1086
4	.0315	.0292	35	.0358	.0321	66	.0893	.0851
5	.0336	.0286	36	-----	-----	67	.0836	.0821
6	.0349	.0267	37	-----	-----	68	.0761	.0716
7	.0276	.0204	38	-----	-----	69	.1467	.1429
8	.0381	.0475	39	-----	-----	70	.0947	.0877
9	.0664	.0718	40	.0549	.0406	71	.0341	.0267
10	.0775	.0821	41	.0536	.0297	72	-.0071	-.0135
11	.0747	.0711	42	.0464	.0200	73	-.0194	-.0268
12	.0571	.0554	43	.0788	.0426	74	-.0206	-.0346
13	.0360	.0317	44	.0478	.0342			
14	.0123	.0043	45	.0438	.0239			
15	-.0054	-.0204	46	.0384	.0136			
16	-.0066	-.0281	47	.0340	.0087			
17	.0073	-.0006	48	.0331	.0117			
18	.0252	.0269	49	.0374	.0223			
19	.0360	.0353	50	.0439	.0334			
20	.0393	.0362	51	.0484	.0391			
21	.0408	.0317	52	.0503	.0403			
22	.0339	.0251	53	.0510	.0423			
23	.0425	.0506	54	.0497	.0392			
24	.0683	.0734	55	.0489	.0356			
25	.0786	.0800	56	.0463	.0266			
26	.0767	.0745	57	.0383	.0211			
27	.0587	.0573	58	.0338	.0294			
28	.0358	.0320	59	.0266	.0251			
29	.0089	.0044	60	.0172	.0094			
30	-.0114	-.0218	61	-----	-----			
31	-.0175	-.0358	62	.0040	-.0013			

TABLE IV.- Continued

(f) $\Delta = 25^\circ$

Orifice no.	C _p at -		Orifice no.	C _p at -		Orifice no.	C _p at -	
	R = 3.3 × 10 ⁶ per m	R = 10 × 10 ⁶ per m		R = 3.3 × 10 ⁶ per m	R = 10 × 10 ⁶ per m		R = 3.3 × 10 ⁶ per m	R = 10 × 10 ⁶ per m
1	-0.0197	-0.0441	32	0.0042	-0.0121	63	0.0573	0.3475
2	-0.0069	-0.0356	33	.0062	-0.0099	64	.0903	.0799
3	.0126	.0123	34	.0186	.0117	65	.1192	.158
4	.0308	.0302	35	.0424	.0305	66	.1053	.1025
5	.0374	.0323	36	-----	-----	67	.1025	.1007
6	.0320	.0207	37	-----	-----	68	.0877	.0878
7	.0196	.0020	38	-----	-----	69	.1444	.1405
8	.0065	-0.0662	39	-----	-----	70	.0940	.0877
9	.0430	.0584	40	.0600	.0476	71	.0310	.0234
10	.0836	.0986	41	.0682	.0507	72	-.0089	-.0162
11	.1012	.1068	42	.0696	.0447	73	-.0201	-.0275
12	.0903	.0905	43	.0940	.0499	74	-.0241	-.0339
13	.0637	.0610	44	.0517	.0289			
14	.0295	.0260	45	.0403	.0189			
15	-.0030	-.0085	46	.0305	.0078			
16	-.0200	-.0194	47	.0245	-.0025			
17	-.0068	-.0353	48	.0244	-.0019			
18	.0130	.0161	49	.0326	.0154			
19	.0309	.0352	50	.0422	.0321			
20	.0418	.0381	51	.0479	.0403			
21	.0376	.0304	52	.056	.0447			
22	.0255	.0098	53	.0535	.0470			
23	.0115	.0008	54	.0538	.0448			
24	.0456	.0648	55	.0564	.0447			
25	.0858	.1005	56	.0605	.0437			
26	.1073	.1097	57	.0597	.0365			
27	.0942	.0688	58	.0509	.0347			
28	.0664	.0610	59	.0371	.0291			
29	.0285	.0256	60	.0211	.0194			
30	-.0045	-.0091	61	-----	-----			
31	-.0243	-.0392	62	-.0038	-.0119			

TABLE IV.- Continued

(g) $A = 300$

Orifice no.	C _p at -		Orifice no.	C _p at -		Orifice no.	C _p at -	
	R = 3.3 × 10 ⁻¹ per m	R = 10 × 10 ⁶ per m		R = 3.3 × 10 ⁶ per m	R = 10 × 10 ⁶ per m		R = 3.3 × 10 ⁶ per m	R = 10 × 10 ⁶ per m
1	-0.0143	-0.0285	32	-0.0013	-0.0138	63	0.0635	0.0537
2	-0.0101	-0.0569	33	-0.0058	-0.0301	64	.0835	.0666
3	.0100	-.0045	34	.0105	.0124	65	.1269	.125
4	.0256	.0275	35	.0298	.0188	66	.1240	.1204
5	.0489	.0452	36	-----	-----	67	.1.96	.1195
6	.0460	.0415	37	-----	-----	68	.0581	.0515
7	.0272	.0107	38	-----	-----	69	.1450	.1388
8	.0048	-.0170	39	-----	-----	70	.0935	.0856
9	.0039	.0014	40	.0548	.0484	71	.0332	.0213
10	.0465	.0571	41	.0639	.0532	72	-.0066	-.0147
11	.0924	.1083	42	.0796	.0624	73	-.0152	-.0237
12	.120 ¹	.1247	43	.1188	.0776	74	-.0187	-.0285
13	.1040	.1038	44	.0822	.0555			
14	.0648	.0609	45	.0627	.0367			
15	.0213	.0150	46	.0389	.0129			
16	-.0144	-.0244	47	.0176	-.0114			
17	-.0119	-.0575	48	.0109	-.0248			
18	.0075	-.0029	49	.0247	-.0038			
19	.0203	.0280	50	.0385	.0211			
20	.0437	.0429	51	.0452	.0320			
21	.0464	.0431	52	.0452	.0360			
22	.0292	.0152	53	.0441	.0367			
23	.0080	-.0118	54	.0463	.0399			
24	.0043	.0059	55	.0533	.0497			
25	.0450	.584	56	.0627	.0584			
26	.0976	.1193	57	.0736	.0612			
27	.1210	.1261	58	.0754	.0586			
28	.1049	.0977	59	.0625	.0459			
29	.0634	.0590	60	.0402	.0272			
30	.0213	.0159	61	-----	-----			
31	-.0115	-.0240	62	-.0067	-.0187			

TABLE IV.- Continued

(h) $\Lambda = 45^\circ$

Orifice no.	C _p at -		Orifice no.	C _p at -		Orifice no.	C _p at -	
	R = 3.3 × 10 ⁶ per sec	R = 10 × 10 ⁶ per sec		R = 3.3 × 10 ⁶ per sec	R = 10 × 10 ⁶ per sec		R = 3.3 × 10 ⁶ per sec	R = 10 × 10 ⁶ per sec
1	0.0246	0.0211	32	-0.0024	-0.0123	63	0.0579	0.0550
2	-.0093	-.0196	33	-.0134	-.0472	64	.0553	.0310
3	-.0062	-.0534	34	.0058	-.0343	65	.1209	.1066
4	.0188	+.0001	35	.0254	.0130	66	.0349	.0580
5	.0367	.0316	36	-----	-----	67	-.0039	.0019
6	.0374	.0393	37	-----	-----	68	-.0091	-.0249
7	.0532	.0491	38	-----	-----	69	.1372	.1346
8	.0565	.0574	39	-----	-----	70	.0841	.0794
9	.0417	.0441	40	.0491	.0427	71	.0314	.0257
10	.0387	.0383	41	.0572	.0523	72	.0077	.0009
11	.0519	.0523	42	.0717	.0693	73	.0089	.0008
12	.0778	.0823	43	.1163	.0953	74	.0199	.0099
13	.0871	.0941	44	.0841	.0772			
14	.0772	.0830	45	.0709	.0598			
15	.0521	.0558	46	.0499	.0349			
16	.0201	.0217	47	.0224	.0022			
17	-.0164	-.0227	48	-.0005	-.0342			
18	-.0105	-.0571	49	.0124	-.0434			
19	.0126	-.0117	50	.0274	.0085			
20	.0285	.0250	51	.0395	.0291			
21	.0285	.0301	52	.0442	.0337			
22	.0429	.0376	53	.0450	.0355			
23	.0507	.0560	54	.0458	.0378			
24	.0422	.0494	55	.0503	.0458			
25	.0372	.0386	56	.0609	.0591			
26	.0512	.0514	57	.0756	.0753			
27	.0702	.0750	58	.0879	.0859			
28	.0786	.0840	59	.0843	.0800			
29	.0659	.0729	60	.0666	.0616			
30	.0403	.0447	61	-----	-----			
31	.0105	.0126	62	.0055	-.0009			

TABLE IV.- Continued

(1) $A = 600$

Orifice no.	C_p at -		Orifice no.	C_p at -		Orifice no.	C_p at -	
	$R = 3.3 \times 10^6$ per sec	$R = 10 \times 10^6$ per sec		$R = 3.3 \times 10^6$ per sec	$R = 10 \times 10^6$ per sec		$R = 3.3 \times 10^6$ per sec	$R = 10 \times 10^6$ per sec
1	0.0121	0.0085	32	0.0112	0.0054	63	0.0435	0.0275
2	-.0282	-.0336	33	-.0248	-.0375	64	.0404	.0146
3	-.0320	-.0714	34	-.0116	-.0536	65	-.0013	.479
4	-.0144	-.0445	35	.0067	-.0086	66	.0007	.0028
5	.0045	-.0035	36	-----	-----	67	.0101	.0015
6	.0123	.0052	37	-----	-----	68	.0253	.0110
7	.0124	.0010	38	-----	-----	69	.0906	.0945
8	.0320	.0258	39	-----	-----	70	.0631	.0607
9	.0621	.0674	40	.0536	.0484	71	.0326	.0273
10	.0872	.1008	41	.0697	.0654	72	.0311	.0259
11	.1181	.1371	42	.0960	.0929	73	.0524	.0495
12	.1274	.1379	43	.1418	.1200	74	.0357	.0336
13	.1173	.1242	44	.1064	.0968			
14	.0927	.0956	45	.0660	.0731			
15	.0564	.0571	46	.0568	.0409			
16	.0153	.0135	47	.0232	.0019			
17	-.0315	-.0369	48	-.0664	-.0371			
18	-.0369	-.0783	49	.0056	-.0473			
19	-.0184	-.0575	50	.0188	-.0045			
20	-.0025	-.0184	51	.0325	.0218			
21	.0056	-.0076	52	.0379	.0282			
22	.0063	-.0071	53	.0382	.0282			
23	.0221	.0145	54	.0421	.0342			
24	.0520	.0577	55	.0539	.0513			
25	.0806	.1085	56	.0690	.0696			
26	.1221	.1574	57	.0895	.0928			
27	.1283	.1484	58	.0980	.1003			
28	.1125	.1240	59	.0887	.0885			
29	.0816	.0855	60	.0644	.0625			
30	.0459	.0438	61	-----	-----			
31	.0074	.2035	62	.0009	-.0047			

TABLE IV.- Continued

(j) $\Delta = 75^\circ$

Orifice no.	C _p at -		Orifice no.	C _p at -		Orifice no.	C _p at -	
	R = 3.3 × 10 ⁶ per sec	R = 10 × 10 ⁶ per sec		R = 3.3 × 10 ⁶ per sec	R = 10 × 10 ⁶ per sec		R = 3.3 × 10 ⁶ per sec	R = 10 × 10 ⁶ per sec
1	0.0154	0.0179	32	0.0178	0.0161	63	0.0317	0.0138
2	-.0300	-.0305	33	-.0252	-.0297	64	.0203	.0165
3	-.0328	-.0709	34	-.0224	-.0612	65	.0254	.0160
4	-.0171	-.0399	35	-.0035	-.0213	66	.0284	.0224
5	.0038	.0023	36	-----	-----	67	.0325	.0273
6	.0138	.0112	37	-----	-----	68	.0372	.0326
7	.0159	.0101	38	-----	-----	69	.0464	.0508
8	.0239	.0179	39	-----	-----	70	.0312	.0250
9	.0437	.0414	40	.0572	.0538	71	.0366	.0373
10	.0690	.0748	41	.0766	.0764	72	.0238	.0255
11	.1104	.1320	42	.1082	.1130	73	.0208	.0224
12	.1368	.1637	43	.1590	.1455	74	.0154	.0142
13	.1314	.1583	44	.1215	.1200			
14	.0989	.1182	45	.0996	.0935			
15	.0536	.0648	46	.0689	.0575			
16	.0071	.0112	47	.0320	.0160			
17	-.0412	-.0443	48	-.0067	-.0278			
18	-.0340	-.0748	49	-.0071	.0591			
19	-.0196	-.0429	50	.0049	-.0224			
20	-.0011	-.0045	51	.0213	.0146			
21	.0079	.0025	52	.0289	.0214			
22	.0107	.0033	53	.0298	.0221			
23	.0207	.0149	54	.0381	.0328			
24	.0419	.0401	55	.0542	.0529			
25	.0666	.0740	56	.0727	.0759			
26	.1124	.1330	57	.1007	.1115			
27	.1291	.1509	58	.1137	.1235			
28	.1203	.1409	59	.1047	.1109			
29	.0836	.1016	60	.0785	.0814			
30	.0401	.0506	61	-----	-----			
31	-.0028	.0034	62	.0061	.0046			

TABLE IV.- Concluded

(k) $\delta = 90^\circ$

Orifice no.	C_p at -		Orifice no.	C_p at -		Orifice no.	γ at -	
	$R = 3.3 \times 10^6$ per sec	$R = 10 \times 10^6$ per sec		$R = 3.3 \times 10^6$ per sec	$R = 10 \times 10^6$ per sec		$R = 3.3 \times 10^6$ per sec	$R = 10 \times 10^6$ per sec
1	0.0151	0.0200	32	0.0144	0.0158	63	0.0275	0.0395
2	-.0307	-.0266	33	-.0296	-.0312	64	.0168	.0490
3	-.0336	-.0653	34	-.0262	-.0673	65	.0230	.0372
4	-.0175	-.0393	35	-.0068	-.0311	66	.0253	.0322
5	.0042	.0121	36	-----	-----	67	.0297	.0235
6	.0145	.0209	37	-----	-----	68	.0340	.0580
7	.0170	.0215	38	-----	-----	69	.0430	.0060
8	.0248	.0326	39	-----	-----	70	.0279	.0073
9	.0448	.0538	40	.0548	.0489	71	.0339	.0053
10	.0697	.0780	41	.0749	.0722	72	.0206	.0025
11	.1117	.1182	42	.1075	.1124	73	.0177	.0156
12	.1380	.1357	43	.1648	.1466	74	.0122	.0105
13	.1331	.1264	44	.1204	.1203			
14	.0998	.0965	45	.0981	.0938			
15	.0541	.0568	46	.0665	.0571			
16	.0070	.0136	47	.0286	.0152			
17	-.0420	-.0357	48	-.0107	-.0268			
18	-.0346	-.0678	49	-.0114	-.0631			
19	-.0200	-.0345	50	.0014	-.0279			
20	-.0018	.0066	51	.0179	.0117			
21	.0077	.0149	52	.0260	.0195			
22	.0111	.0163	53	.0268	.0207			
23	.0212	.0264	54	.0350	.0317			
24	.0434	.0497	55	.0522	.0517			
25	.0690	.0735	56	.0711	.0735			
26	.1150	.1149	57	.0991	.1095			
27	.1292	.1272	58	.1127	.1224			
28	.1213	.1143	59	.1040	.1121			
29	.0847	.0835	60	.0766	.0819			
30	.0413	.0438	61	-----	-----			
31	-.0030	.0036	62	.0026	.0047			

TABLE V.- PRESSURE COEFFICIENT DATA AT $M_{\infty} = 2.4$ AND $\delta = 12.7$ cm(a) $\Delta = 0^\circ$

Orifice no.	C_p at -		Orifice no.	C_p at -		Orifice no.	C_p at -	
	$R = 3.3 \times 10^6$ per sec	$R = 10 \times 10^6$ per sec		$R = 3.3 \times 10^6$ per sec	$R = 10 \times 10^6$ per sec		$R = 3.3 \times 10^6$ per sec	$R = 10 \times 10^6$ per sec
1	0.0114	0.0073	32	0.0050	-0.0001	63	0.0404	0.0269
2	.0561	.0061	33	.0009	-.0002	64	.0694	.0731
3	.081	.0061	34	.0000	-.0032	65	.0351	.0391
4	.085	.0060	35	-.0001	-.0028	66	.0084	.0044
5	.078	.0052	36	.0011	-.0007	67	.0078	.0047
6	.0078	.0049	37	-.0001	-.0032	68	.0102	.0034
7	.0077	.0047	38	.0005	-.0016	69	.0792	.0842
8	.0077	.0046	39	.0000	-.0026	70	.0396	.0346
9	.0079	.0049	40	.0008	-.0018	71	.0171	.0133
10	.0082	.0054	41	.0007	-.0017	72	.0124	.0127
11	.0075	.0049	42	.0004	-.0015	73	.0134	.0117
12	.0084	.0058	43	.0002	-.0018	74	.0098	.0058
13	.0082	.0061	44	.0007	-.0004			
14	.0078	.0056	45	.0010	.0006			
15	.0079	.0070	46	.0010	-.0002			
16	.0084	.0072	47	.0014	.0001			
17	.0064	.0058	48	.0016	.0002			
18	.0063	.0057	49	.0029	.0023			
19	.0051	.0032	50	.0022	.0010			
20	.0541	.0028	51	.0024	.0010			
21	.0035	.0016	52	.0032	.0018			
22	.0036	.0023	53	.0041	.0028			
23	.0028	.0014	54	.0031	.0008			
24	.0022	.0004	55	.0033	.0011			
25	.0027	.0005	56	.0044	.0025			
26	.0029	.0005	57	.0037	.0017			
27	.0032	.0013	58	.0041	.0026			
28	.0034	.0017	59	.0045	.003			
29	.0034	.0024	60	.0042	.0020			
30	.0039	.0028	61	.0045	.0027			
31	.0049	.0036	62	.0050	.0033			

TABLE V.- Continued

(b) $\Lambda = -50$

Orifice no.	C _p at -		Orifice no.	C _p at -		Orifice no.	C _p at -	
	R = 3.3 × 10 ⁶ per m	R = 10 × 10 ⁶ per m		R = 3.3 × 10 ⁶ per m	R = 10 × 10 ⁶ per m		R = 3.3 × 10 ⁶ per m	R = 10 × 10 ⁶ per m
1	0.0096	0.0039	32	0.0027	-0.0031	63	0.0444	0.0272
2	.0062	.0026	33	-.0010	-.0025	64	.0728	.0721
3	.0066	.0030	34	-.0011	-.0049	65	.0402	.0407
4	.0072	.0040	35	-.0003	-.0032	66	.0135	.0085
5	.0075	.0045	36	.0022	.0005	67	.0116	.0057
6	.0103	.0055	37	.0038	-.0010	68	.0129	.0019
7	.0123	.0066	38	.0065	.0018	69	.0837	.0838
8	.0119	.0066	39	.0058	.0005	70	.0424	.0345
9	.0118	.0072	40	.0062	.0013	71	.0153	.0078
10	.0114	.0072	41	.0057	.0011	72	.0115	.0061
11	.0102	.0058	42	.0051	.0008	73	.0155	.0103
12	.0100	.0056	43	.0043	.0004	74	.0124	.0062
13	.0090	.0051	44	.0041	.0014			
14	.0078	.0030	45	.0038	.0005			
15	.0077	.0027	46	.0041	.0007			
16	.0075	.0017	47	.0045	.0007			
17	.0054	.0002	48	.0048	.0009			
18	.0054	.0002	49	.0064	.0027			
19	.0052	-.0010	50	.0069	.0025			
20	.0059	.0001	51	.0080	.0032			
21	.0066	.0006	52	.0098	.0051			
22	.0071	.0028	53	.0103	.0064			
23	.0066	.0020	54	.0091	.0038			
24	.0066	.0015	55	.0090	.0039			
25	.0069	.0019	56	.0096	.0045			
26	.0072	.0017	57	.0084	.0031			
27	.0071	.0022	58	.0078	.0029			
28	.0073	.0023	59	.0074	.0025			
29	.0070	.0022	60	.0070	.0016			
30	.0069	.0015	61	.0064	.0015			
31	.0074	.0019	62	.0067	.0020			

TABLE V.- Continued

(c) $\Delta = -10^0$

Orifice no.	C _p at -		Orifice no.	C _p at -		Orifice no.	C _p at -	
	R = 3.3 x 10 ⁶ per m	R = 10 x 10 ⁶ per m		R = 3.3 x 10 ⁶ per m	R = 10 x 10 ⁶ per m		R = 3.3 x 10 ⁶ per m	R = 10 x 10 ⁶ per m
1	0.0034	-0.0032	32	-0.0007	-0.0060	63	0.0394	0.0271
2	.0003	-.0031	33	-.0034	-.0045	64	.0692	.0716
3	.0002	-.0004	34	-.0060	-.0057	65	.0421	.0456
4	.0019	.0029	35	-.0053	-.0019	66	.0172	.0165
5	.0019	.0053	36	-.0030	.0043	67	.0118	.0108
6	.0088	.0090	37	.0046	.0048	68	.0099	.0010
7	.0092	.0117	38	.0043	.0084	69	.0795	.0820
8	.0066	.0101	39	.0000	.0064	70	.0373	.0343
9	.0104	.0096	40	.0071	.0066	71	.0050	-.0007
10	.0093	.0082	41	.0066	.0061	72	-.0010	-.0092
11	.0071	.0052	42	.0055	.0049	73	.0070	.0042
12	.0059	.0028	43	.0038	.0030	74	.0069	.0064
13	.0032	-.0003	44	.0021	.0020			
14	.0004	-.0041	45	.0004	-.0002			
15	-.0014	-.0055	46	-.0007	-.0021			
16	-.0017	-.0061	47	-.0010	-.0030			
17	-.0025	-.0058	48	-.0002	-.0024			
18	-.0010	-.0034	49	.0024	.0008			
19	.0009	-.0017	50	.0043	.0026			
20	.0040	.0023	51	.0071	.0057			
21	.0072	.0057	52	.0104	.0098			
22	.0097	.0098	53	.0113	.0115			
23	.0090	.0078	54	.0099	.0085			
24	.0082	.0068	55	.0094	.0084			
25	.0073	.0062	56	.0094	.0082			
26	.0060	.0043	57	.0072	.0060			
27	.0048	.0031	58	.0058	.0045			
28	.0032	.0004	59	.0042	.0020			
29	.0007	-.0019	60	.0020	-.0007			
30	-.0007	-.0033	61	.0006	-.0020			
31	-.0003	-.0028	62	.0008	-.0022			

TABLE V.- Continued

(d) $\Lambda = -15^\circ$

Orifice no.	C _p at -		Orifice no.	C _p at -		Orifice no.	C _p at -	
	R = 3.3 × 10 ⁶ per m	R = 10 × 10 ⁶ per m		R = 3.3 × 10 ⁶ per m	R = 10 × 10 ⁶ per m		R = 3.3 × 10 ⁶ per m	R = 10 × 10 ⁶ per m
1	-0.0032	-0.0093	32	-0.0034	-0.0099	63	0.0407	0.0313
2	-.0054	-.0083	33	-.0059	-.0079	64	.0723	.0717
3	-.0022	-.0043	34	-.0030	-.0071	65	.0489	.0536
4	.0027	.0004	35	.0020	-.0004	66	.0266	.0280
5	.0082	.0063	36	.0088	.0090	67	.0205	.0222
6	.0149	.0132	37	.0125	.0120	68	.0150	.0081
7	.0177	.0176	38	.0152	.0163	69	.0804	.0822
8	.0153	.0142	39	.0134	.0140	70	.0362	.0340
9	.0127	.0123	40	.0131	.0136	71	-.0030	-.0077
10	.0103	.0091	41	.0116	.0119	72	-.0134	-.0268
11	.0080	.0059	42	.0097	.0100	73	-.0035	-.0139
12	.0056	.0026	43	.0065	.0067	74	.0013	-.0013
13	.0018	-.0022	44	.0027	.0024			
14	-.0027	-.0078	45	-.0014	-.0035			
15	-.0058	-.0099	46	-.0042	-.0070			
16	-.0063	-.0106	47	-.0050	-.0090			
17	-.0062	-.0091	48	-.0039	-.0074			
18	-.0025	-.0054	49	.0006	-.0021			
19	.0025	-.0007	50	.0053	.0032			
20	.0093	.0063	51	.0107	.0095			
21	.0162	.0134	52	.0166	.0165			
22	.0198	.0197	53	.0182	.0188			
23	.0168	.0156	54	.0162	.0153			
24	.0142	.0124	55	.0153	.0144			
25	.0119	.0103	56	.0140	.0136			
26	.0101	.0080	57	.0113	.0109			
27	.0075	.0050	58	.0084	.0078			
28	.0038	.0003	59	.0045	.0024			
29	-.0012	-.0047	60	-.0003	-.0039			
30	-.0038	-.0073	61	-.0033	-.0076			
31	-.0043	-.0066	62	-.0040	-.0077			

TABLE V. - Continued

(e) $\Lambda = -20^\circ$

Orifice no.	C _p at -		Orifice no.	C _p at -		Orifice no.	C _p at -	
	R = 3.3 × 10 ⁶ per m	R = 10 × 10 ⁶ per m		R = 3.3 × 10 ⁶ per m	R = 10 × 10 ⁶ per m		R = 3.3 × 10 ⁶ per m	R = 10 × 10 ⁶ per m
1	-0.0106	-0.0208	32	-0.0087	-0.0196	63	0.0414	0.0304
2	-0.0139	-0.0226	33	-0.0108	-0.0168	64	.0698	.0681
3	-0.0088	-0.0182	34	-0.0055	-0.0121	65	.0571	.0597
4	.0000	-0.0088	35	.0031	-0.0008	66	.0385	.0389
5	.0104	.0048	36	.0143	.0141	67	.0324	.0337
6	.0221	.0194	37	.0209	.0202	68	.0253	.0195
7	.0250	.0266	38	.0234	.0241	69	.0815	.0785
8	.0198	.0210	39	.0204	.0203	70	.0327	.0284
9	.0134	.0150	40	.0181	.0174	71	-.0115	-.0167
10	.0105	.0098	41	.0143	.0143	72	-.0279	-.0421
11	.009 ^h	.0096	42	.0118	.0127	73	-.0206	-.0434
12	.0073	.0065	43	.0081	.0082	74	-.0119	-.0303
13	.0026	.0005	44	.0020	.0015			
14	-.0042	-.0092	45	-.0047	-.0089			
15	-.0104	-.0168	46	-.0099	-.0164			
16	-.0130	-.0219	47	-.0123	-.0198			
17	-.0133	-.0232	48	-.0105	-.0179			
18	-.0072	-.0174	49	-.0033	-.0088			
19	.0021	-.0071	50	.0054	.0020			
20	.0141	.0073	51	.0152	.0133			
21	.0250	.0217	52	.0242	.0236			
22	.0284	.0307	53	.0252	.0259			
23	.0219	.0242	54	.0216	.0209			
24	.0146	.0160	55	.0186	.0181			
25	.0120	.0111	56	.0154	.0156			
26	.0118	.0127	57	.0122	.0135			
27	.0093	.0100	58	.0085	.0100			
28	.0037	.0044	59	.0023	.0021			
29	-.0043	-.0045	60	-.0053	-.0083			
30	-.0104	-.0127	61	-.0107	-.0151			
31	-.0137	.0170	62	-.0118	-.0168			

TABLE V.- Continued

(f) $\Delta = -30^\circ$

Orifice no.	C _p at -		Orifice no.	C _p at -		Orifice no.	C _p at -	
	R = 3.3 × 10 ⁶ per m	R = 10 × 10 ⁶ per m		R = 3.3 × 10 ⁶ per m	R = 10 × 10 ⁶ per m		R = 3.3 × 10 ⁶ per m	R = 10 × 10 ⁶ per m
1	-0.0190	-0.0545	32	-0.0183	-0.0396	63	0.0389	0.0327
2	-0.0196	-0.0373	33	-0.0159	-0.0272	64	.0638	.0610
3	.0004	-0.0080	34	-0.0028	-0.0098	65	.0706	.0777
4	.0250	.0224	35	.0131	.0127	66	.0627	.0681
5	.0434	.0495	36	.0285	.0355	67	.0598	.0672
6	.0449	.0624	37	.0336	.0405	68	.0463	.0530
7	.0288	.0463	38	.0320	.0394	69	.0776	.0800
8	.0090	.0148	39	.0267	.0303	70	.0212	.0210
9	.0060	-.0042	40	.0232	.0243	71	-.0255	-.0268
10	.0124	.0101	41	.0191	.0193	72	-.0467	-.0533
11	.0175	.0227	42	.0165	.0178	73	-.0423	-.0622
12	.0142	.0196	43	.0113	.0138	74	-.0295	-.0640
13	.0023	.0072	44	.0029	.0045			
14	-.0039	-.0103	45	-.0088	-.0151			
15	-.0118	-.0436	46	-.0192	-.0360			
16	-.0213	-.0555	47	-.0237	-.0418			
17	-.0174	-.0336	48	-.0173	-.0298			
18	.0037	-.0039	49	-.0003	-.0054			
19	.0281	.0263	50	.0162	.0165			
20	.0468	.0538	51	.0280	.0331			
21	.0476	.0659	52	.0344	.0439			
22	.0314	.0516	53	.0308	.0389			
23	.0120	.0210	54	.0245	.0288			
24	.0082	-.0033	55	.0196	.0219			
25	.0133	.0058	56	.0165	.0167			
26	.0182	.0215	57	.0144	.0139			
27	.0171	.0222	58	.0115	.0103			
28	.0065	.0145	59	.0054	.0030			
29	-.0027	-.0054	60	-.0041	-.0100			
30	-.0113	-.0419	61	-.0126	-.0232			
31	-.0217	-.0523	62	-.0164	-.0284			

31

TABLE V.- Continued

(g) $\Delta = -45^\circ$

Orifice no.	C _p at -		Orifice no.	C _p at -		Orifice no.	C _p at -	
	R = 3.3 × 10 ⁶ per m	R = 10 × 10 ⁶ per m		R = 3.3 × 10 ⁶ per m	R = 10 × 10 ⁶ per m		R = 3.3 × 10 ⁶ per m	R = 10 × 10 ⁶ per m
1	-0.0047		32	-0.0141		63	-0.0248	-0.0399
2	.0143		33	.0153		64	-.0125	.0573
3	.0317		34	.0364		65	.0102	.0893
4	.0374		35	.0427		66	.0274	.0623
5	.0291		36	.0337		67	.0413	.0707
6	.0158		37	.0177		68	.0475	-.0123
7	.0146		38	.0139		69	.0399	-.0159
8	.0215		39	.0249		70	.0320	.0565
9	.0308		40	.0389		71	.0240	.0611
10	.0319		41	.0418		72	.0209	-.0005
11	.0199		42	.0155		73	.0213	.0002
12	.0154		43	.0090		74	.0166	-.0361
13	.0078		44	-.0088		75	-.0019	-.0497
14	-.0064		45	-.0444		76	-.0152	-.0505
15	-.0211		46	-.0483		77	-.0272	-.0424
16	-.0092		47	-.0164		78	-.0319	-.0489
17	.0140		48	.0171		79	-.0151	-.0212
18	.0328		49	.0399		80	.0151	.0154
19	.0388		50	.0454		81	.0416	.0473
20	.0330		51	.0371		82	.0579	.0677
21	.0179		52	.0207		83	.0605	.0742
22	.0126		53	.0125		84	.0436	.0558
23	.0151		54	.0186		85	.0273	.0296
24	.0236		55	.0320		86	.0144	.0123
25	.0282		56	.0331		87	.0095	.0051
26	.0215		57	.0166		88	.0081	.0057
27	.0162		58	.0151		89	.0038	.0026
28	.0090		59	.0004		90	-.0064	-.0105
29	-.0052		60	-.0362		91	.0203	-.0447
30	-.0177		61	-.0449		92	-.0348	-.0629
31	-.0098		62	-.0142		93	-.0308	-.0372

32

TABLE V.- Continued

(h) $\Lambda = -60^\circ$

Orifice no.	C _p at -		Orifice no.	C _p at -		Orifice no.	C _p at -	
	R = 3.3 × 10 ⁶ per m	R = 10 × 10 ⁶ per m		R = 3.3 × 10 ⁶ per m	R = 10 × 10 ⁶ per m		R = 3.3 × 10 ⁶ per m	R = 10 × 10 ⁶ per m
1	-0.0220	-0.0272	32	-0.0266	-0.0353	63	0.0091	0.0036
2	.0028	.0014	33	-.0057	-.0028	64	.0480	.0137
3	.0317	.0331	34	.0213	.0270	65	.0187	.0363
4	.0553	.0593	35	.0451	.0546	66	-.0090	-.0114
5	.0691	.0793	36	.0615	.0758	67	-.0032	-.0059
6	.0739	.0919	37	.0591	.0734	68	.0126	.0064
7	.0594	.0802	38	.0438	.0448	69	.0237	.0248
8	.0458	.0581	39	.0295	.0357	70	-.0123	-.0134
9	.0289	.0336	40	.0175	.0190	71	-.0304	-.0305
10	.0106	.0032	41	.0092	.0087	72	-.0257	-.0272
11	.0036	-.0050	42	.0059	.0063	73	-.0071	-.0093
12	-.0058	-.0161	43	-.0011	.0000	74	-.0113	-.0107
13	-.0205	-.0468	44	-.0145	-.0171			
14	-.0349	-.0751	45	-.0280	-.0551			
15	-.0475	-.0634	46	-.0435	-.0646			
16	-.0305	-.0343	47	-.0330	-.0350			
17	-.0014	-.0007	48	-.0039	-.0003			
18	.0262	.0280	49	.0301	.0378			
19	.0468	.0522	50	.0556	.0666			
20	.0589	.0688	51	.0679	.0806			
21	.0607	.0740	52	.0651	.0794			
22	.0494	.0625	53	.0453	.0546			
23	.0396	.0472	54	.0301	.0352			
24	.0276	.0292	55	.0172	.0190			
25	.0137	.0077	56	.0092	.0098			
26	.0068	.0004	57	.0064	.0084			
27	-.0012	-.0073	58	-.0004	.0035			
28	-.0156	-.0328	59	-.0136	-.0184			
29	-.0318	-.0685	60	-.0274	-.0556			
30	-.0451	-.0657	61	-.0425	-.0568			
31	-.0297	-.0322	62	-.0237	-.0205			

TABLE V.- Concluded

(i) $\Lambda = -90^\circ$

Orifice no.	C _p at -		Orifice no.	C _p at -		Orifice no.	C _p at -	
	R = 3.3 × 10 ⁶ per m	R = 10 × 10 ⁶ per m		R = 3.3 × 10 ⁶ per m	R = 10 × 10 ⁶ per m		R = 3.3 × 10 ⁶ per m	R = 10 × 10 ⁶ per m
1	-0.0191	-0.0213	32	-0.0209	-0.0230	63	0.0349	0.0308
2	.0096	.0104	33	.0062	.0117	64	.0676	.0355
3	.0428	.0482	34	.0374	.0450	65	.0305	.0279
4	.0685	.0759	35	.0635	.0744	66	.0300	.0281
5	.0815	.0926	36	.0778	.0911	67	.0267	.0209
6	.0779	.0890	37	.0734	.0859	68	.0366	.0407
7	.0542	.0602	38	.0519	.0588	69	-.0323	-.0360
8	.0368	.0387	39	.0349	.0375	70	-.0307	-.0318
9	.0207	.0192	40	.0196	.0187	71	-.0272	-.0274
10	.0080	.0058	41	.0078	.0057	72	-.0285	-.0312
11	.0026	.0023	42	.0029	.0034	73	-.0279	-.0271
12	-.0071	-.0044	43	-.0059	-.0029	74	-.0314	-.0354
13	-.0237	-.0342	44	-.0230	-.0314			
14	-.u 55	-.0680	45	-.0367	-.0665			
15	-.0411	-.0556	46	-.0504	-.0501			
16	-.0207	-.0202	47	-.0277	-.0240			
17	.0173	.0213	48	.0068	.0143			
18	.0510	.0555	49	.0436	.0547			
19	.0775	.0863	50	.0719	.0862			
20	.0898	.1009	51	.0829	.0990			
21	.0836	.0962	52	.0765	.0913			
22	.0576	.0635	53	.0523	.0596			
23	.0392	.0410	54	.0344	.0373			
24	.0216	.0210	55	.0180	.0180			
25	.0079	.0067	56	.0056	.0046			
26	.0034	.0047	57	.0008	.0023			
27	-.0049	-.0023	58	-.0071	-.0035			
28	-.0202	-.0312	59	-.0227	-.0318			
29	-.0352	-.0657	60	-.0358	-.0666			
30	-.0437	-.0499	61	-.0466	-.0512			
31	-.0115	-.0088	62	-.0178	-.0112			

TABLE VI.- PRESSURE COEFFICIENT DATA AT $M_{\infty} = 4.5$, $\delta = 12.7$ cm,AND $R = 10 \times 10^6$ PER METER(a) $\Lambda = 0^\circ$

Orifice no.	C_p	Orifice no.	C_p	Orifice no.	C_p
1	0.0021	32	0.0036	63	0.0022
2	-.0019	33	-.0024	64	.0210
3	-.0018	34	-.0028	65	.0191
4	-.0013	35	-.0025	66	.0085
5	-.0012	36	-.0020	67	.0016
6	-.0009	37	-.0020	68	-.0003
7	-.0009	38	-.0017	69	.0328
8	-.0009	39	-.0019	70	.0156
9	-.0008	40	-.0018	71	.0007
10	-.0007	41	-.0018	72	-.0023
11	-.0012	42	-.0020	73	.0030
12	-.0013	43	-.0021	74	.0040
13	-.0014	44	-.0018		
14	-.0017	45	.0010		
15	-.0013	46	-.0017		
16	-.0009	47	-.0019		
17	-.0010	48	-.0018		
18	-.0003	49	-.0013		
19	-.0001	50	-.0015		
20	.0003	51	-.0013		
21	.0005	52	-.0009		
22	.0008	53	-.0006		
23	.0005	54	-.0009		
24	.0004	55	-.0009		
25	.0007	56	-.0004		
26	.0004	57	-.0009		
27	.0005	58	-.0006		
28	.0003	59	-.0004		
29	.0000	60	-.0004		
30	.0000	61	-.0004		
31	.0000	62	-.0006		

TABLE VI.- Continued

(b) $\Lambda = -5^\circ$

Orifice no.	C_p	Orifice no.	C_p	Orifice no.	C_p
1	0.0017	32	0.0025	63	0.0022
2	-.0024	33	-.0034	64	.0194
3	-.0022	34	-.0035	65	.0180
4	-.0018	35	-.0028	66	.0090
5	-.0013	36	-.0013	67	.0035
6	-.0005	37	-.0009	68	.0021
7	-.0001	38	-.0006	69	.0309
8	-.0001	39	-.0010	70	.0145
9	-.0002	40	-.0011	71	.0006
10	-.0005	41	-.0013	72	-.0041
11	-.0013	42	-.0019	73	-.0014
12	-.0013	43	-.0023	74	-.0006
13	-.0011	44	-.0025		
14	-.0019	45	-.0031		
15	-.0017	46	-.0033		
16	-.0014	47	-.0035		
17	-.0015	48	-.0032		
18	-.0011	49	-.0022		
19	-.0007	50	-.0015		
20	-.0001	51	-.0006		
21	.0007	52	.0005		
22	.0014	53	.0010		
23	.0007	54	.0003		
24	.0006	55	.0002		
25	.0002	56	.0003		
26	-.0001	57	-.0003		
27	-.0003	58	-.0006		
28	-.0006	59	-.0009		
29	-.0008	60	-.0013		
30	-.0010	61	-.0017		
31	-.0008	62	-.0016		

TABLE VI.- Continued

(c) $\Lambda = -10^\circ$

Orifice no.	C_p	Orifice no.	C_p	Orifice no.	C_p
1	-0.0018	32	0.0001	63	0.0019
2	-.0064	33	-.0055	64	.0171
3	-.0058	34	-.0047	65	.0173
4	-.0036	35	-.0026	66	.0107
5	-.0013	36	-.0004	67	.0071
6	.0018	37	.0004	68	.0010
7	.0032	38	.0004	69	.0294
8	.0028	39	.0000	70	.0135
9	.0019	40	.0001	71	-.0002
10	.0003	41	-.0007	72	-.0070
11	-.0002	42	-.0012	73	-.0071
12	-.0007	43	-.0021	74	-.0062
13	.0001	44	-.0030		
14	-.0030	45	-.0045		
15	-.0047	46	-.0056		
16	-.0055	47	-.0057		
17	-.0061	48	-.0051		
18	-.0049	49	-.0029		
19	-.0028	50	-.0007		
20	-.0003	51	.0011		
21	.0026	52	.0027		
22	.0041	53	.0027		
23	.0034	54	.0021		
24	.0024	55	.0020		
25	.0005	56	.0018		
26	.0003	57	.0010		
27	-.0003	58	.0001		
28	-.0011	59	-.0011		
29	-.0025	60	-.0027		
30	-.0038	61	-.0039		
31	-.0049	62	-.0038		

TABLE VI.- Continued

(d) $\Lambda = -15^\circ$

Orifice no.	C_p	Orifice no.	C_p	Orifice no.	C_p
1	-0.0062	32	-0.0013	63	0.0023
2	-.0101	33	-.0062	64	.0149
3	-.0070	34	-.0042	65	.0171
4	-.0020	35	-.0013	66	.0137
5	.0031	36	.0011	67	.0118
6	.0079	37	.0010	68	.0106
7	.0089	38	.0009	69	.0279
8	.0065	39	.0010	70	.0127
9	.0008	40	.0014	71	-.0011
10	-.0023	41	.0006	72	-.0095
11	-.0019	42	-.0002	73	-.0109
12	-.0024	43	-.0015	74	-.0097
13	-.0035	44	-.0028		
14	-.0062	45	-.0051		
15	-.0089	46	-.0070		
16	-.0105	47	-.0074		
17	-.0101	48	-.0058		
18	-.0061	49	-.0021		
19	-.0013	50	.0006		
20	.0038	51	.0023		
21	.0082	52	.0033		
22	.0095	53	.0038		
23	.0071	54	.0039		
24	.0015	55	.0035		
25	-.0025	56	.0029		
26	-.0017	57	.0017		
27	-.0020	58	.0005		
28	-.0027	59	-.0010		
29	-.0052	60	-.0037		
30	-.0077	61	-.0056		
31	-.0092	62	-.0061		

TABLE VI.- Continued

(e) $\Lambda = -20^\circ$

Orifice no.	C_p	Orifice no.	C_p	Orifice no.	C_p
1	-0.0083	32	-0.0014	63	0.0025
2	-.0100	33	-.0050	64	.0126
3	-.0038	34	-.0024	65	.0173
4	.0046	35	.0008	66	.0175
5	.0118	36	.0034	67	.0164
6	.0158	37	.0038	68	.0145
7	.0119	38	.0039	69	.0269
8	.0027	39	.0028	70	.0124
9	-.0057	40	.0032	71	-.0017
10	-.0055	41	.0009	72	-.0109
11	-.0035	42	.0000	73	-.0125
12	-.0032	43	-.0012	74	-.0118
13	-.0056	44	-.0032		
14	-.0079	45	-.0058		
15	-.0109	46	-.0079		
16	-.0128	47	-.0078		
17	-.0098	48	-.0052		
18	-.0029	49	-.0007		
19	.0052	50	.0030		
20	.0125	51	.0056		
21	.0169	52	.0070		
22	.0137	53	.0063		
23	.0045	54	.0044		
24	-.0051	55	.0029		
25	-.0051	56	.0021		
26	-.0024	57	.0015		
27	-.0021	58	.0005		
28	-.0040	59	-.0014		
29	-.0069	60	-.0042		
30	-.0099	61	-.0066		
31	-.0113	62	-.0064		

TABLE VI.- Continued

(f) $\Lambda = -30^\circ$

Orifice no.	C_p	Orifice no.	C_p	Orifice no.	C_p
1	-0.0045	32	-0.0025	63	0.0032
2	.0012	33	-.0033	64	.0399
3	.0122	34	.0028	65	.0184
4	.0187	35	.0084	66	.0208
5	.0144	36	.0121	67	.0079
6	.0025	37	.0115	68	-.0038
7	-.0044	38	.0089	69	.0236
8	-.0072	39	.0060	70	.0105
9	-.0051	40	.0046	71	-.0033
10	-.0030	41	-.0007	72	-.0106
11	-.0038	42	-.0024	73	-.0120
12	-.0061	43	-.0040	74	-.0119
13	-.0064	44	-.0062		
14	-.0075	45	-.0094		
15	-.0114	46	-.0130		
16	-.0084	47	-.0101		
17	.0027	48	-.0033		
18	.0151	49	.0047		
19	.0216	50	.0095		
20	.0176	51	.0110		
21	.0056	52	.0102		
22	-.0017	53	.0071		
23	-.0080	54	.0049		
24	-.0032	55	.0033		
25	-.0016	56	.0018		
26	-.0017	57	.0003		
27	-.0042	58	-.0017		
28	-.0050	59	-.0043		
29	-.0070	60	-.0075		
30	-.0111	61	-.0111		
31	-.0068	62	-.0094		

TABLE VI.- Continued

(g) $\Lambda = -45^\circ$

Orifice no.	C_p	Orifice no.	C_p	Orifice no.	C_p
1	-0.0014	32	-0.0005	63	0.0032
2	.0026	33	.0019	64	.0096
3	.0107	34	.0094	65	.0085
4	.0166	35	.0155	66	-.0116
5	.0177	36	.0186	67	-.0129
6	.0140	37	.0149	68	-.0064
7	.0076	38	.0087	69	.0192
8	.0043	39	.0041	70	.0069
9	.0001	40	.0006	71	-.0026
10	-.0041	41	-.0012	72	-.0073
11	-.0058	42	-.0021	73	-.0058
12	-.0076	43	-.0037	74	-.0014
13	-.0103	44	-.0061		
14	-.0155	45	-.0098		
15	-.0140	46	-.0131		
16	-.0053	47	-.0071		
17	.0047	48	.0027		
18	.0138	49	.0133		
19	.0197	50	.0201		
20	.0204	51	.0217		
21	.0160	52	.0181		
22	.0082	53	.0106		
23	.0044	54	.0050		
24	.0011	55	.0011		
25	-.0037	56	-.0008		
26	-.0058	57	-.0017		
27	-.0073	58	-.0029		
28	-.0100	59	-.0051		
29	-.0150	60	-.0092		
30	-.0136	61	-.0113		
31	-.0050	62	-.0023		

TABLE VI.- Continued

(h) $\Lambda = -60^\circ$

Orifice no.	C_p	Orifice no.	C_p	Orifice no.	C_p
1	0.0000	32	0.0037	63	0.0004
2	.0056	33	.0088	64	.0088
3	.0162	34	.0184	65	-.0102
4	.0256	35	.0260	66	-.0083
5	.0306	36	.0292	67	-.0026
6	.0268	37	.0236	68	.0023
7	.0133	38	.0139	69	.0102
8	.0038	39	.0067	70	.0036
9	-.0036	40	.0008	71	-.0019
10	-.0070	41	-.0023	72	.0013
11	-.0082	42	-.0034	73	.0009
12	-.0098	43	-.0047	74	-.0028
13	-.0118	44	-.0068		
14	-.0168	45	-.0116		
15	-.0147	46	-.0119		
16	-.0050	47	-.0016		
17	.0067	48	.0107		
18	.0182	49	.0234		
19	.0281	50	.0318		
20	.0322	51	.0331		
21	.0276	52	.0277		
22	.0127	53	.0161		
23	.0031	54	.0083		
24	-.0043	55	.0020		
25	-.0080	56	-.0014		
26	-.0086	57	-.0020		
27	-.0097	58	-.0034		
28	-.0112	59	-.0052		
29	-.0168	60	-.0109		
30	-.0141	61	-.0093		
31	-.0018	62	.0029		

TABLE VI.- Concluded

(i) $\Lambda = -90^\circ$

Orifice no.	C_p	Orifice no.	C_p	Orifice no.	C_p
1	0.0025	32	0.0066	63	0.0060
2	.0094	33	.0132	64	.0079
3	.0199	34	.0241	65	.0033
4	.0279	35	.0330	66	.0039
5	.0304	36	.0359	67	.0017
6	.0258	37	.0299	68	.0078
7	.0148	38	.0174	69	-.0077
8	.0072	39	.0086	70	-.0059
9	.0005	40	.0010	71	-.0049
10	-.0043	41	-.0045	72	-.0046
11	-.0059	42	-.0060	73	-.0034
12	-.0076	43	-.0072	74	-.0039
13	-.0091	44	-.0088		
14	-.0141	45	-.0147		
15	-.0123	46	-.0111		
16	-.0012	47	.0011		
17	.0123	48	.0148		
18	.0235	49	.0289		
19	.0318	50	.0392		
20	.0336	51	.0408		
21	.0281	52	.0340		
22	.0159	53	.0193		
23	.0078	54	.0097		
24	.0004	55	.0011		
25	-.0047	56	-.0047		
26	-.0060	57	-.0059		
27	-.0070	58	-.0067		
28	-.0084	59	-.0081		
29	-.0145	60	-.0148		
30	-.0111	61	-.0082		
31	.0018	62	.0054		

TABLE VII.- EXPERIMENTAL HEAT-TRANSFER COEFFICIENTS

(a) $\Lambda = 0^\circ$

Thermocouple no.	h, $\text{W/m}^2\text{-K}$, at -		
	$M_\infty = 2.4$		$M_\infty = 4.5$ $R = 10 \times 10^6 \text{ per m}$
	$R = 3.3 \times 10^6 \text{ per m}$	$R = 10 \times 10^6 \text{ per m}$	
1	26.78	62.14	15.53
2	26.78	62.75	15.53
3	26.98	63.57	15.33
4	28.62	68.06	16.35
5	30.46	72.15	18.19
6	31.07	73.79	18.80
7	32.30	75.63	19.83
8	32.70	76.45	20.24
9	31.68	76.45	20.03
10	31.68	75.63	19.62
11	30.46	73.38	18.19
12	28.00	67.25	17.58
13	25.75	60.91	15.94
14	24.94	59.48	15.13
15	25.75	60.50	16.15
16	25.55	62.14	16.35
17	25.35	61.12	16.35
18	25.96	61.52	15.94
19	27.80	66.84	17.58
20	30.05	71.95	18.60
21	31.07	73.79	19.42
22	32.29	75.83	20.64
23	32.50	77.06	21.05
24	32.50	77.06	20.85
25	31.68	75.42	19.62
26	30.28	72.36	19.83
27	28.20	66.84	17.78
28	24.94	58.25	15.53
29	24.94	58.87	15.33
30	26.37	62.34	16.56

TABLE VII.- Continued

(b) $\Lambda = 5^{\circ}$

Thermocouple no.	$h, \text{W/m}^2\text{-K}, \text{at } -$		
	$M_{\infty} = 2.4$		$M_{\infty} = 4.5$ $R = 10 \times 10^6 \text{ per m}$
	$R = 3.3 \times 10^6 \text{ per m}$	$R = 10 \times 10^6 \text{ per m}$	
1	28.62	66.43	15.13
2	27.19	63.36	13.90
3	25.96	60.50	12.67
4	27.59	63.57	13.90
5	29.64	69.09	15.94
6	30.46	72.15	15.33
7	31.89	74.81	16.97
8	30.66	75.83	17.58
9	32.70	75.83	16.97
10	31.89	73.79	17.58
11	31.68	71.95	17.78
12	29.84	68.68	18.19
13	28.21	63.77	17.78
14	27.19	63.16	16.66
15	27.80	65.61	16.35
16	28.21	66.63	15.53
17	27.39	61.52	15.33
18	25.96	60.09	13.69
19	28.00	64.39	14.92
20	29.84	69.29	16.35
21	31.27	72.77	16.97
22	32.09	75.42	17.99
23	32.50	74.81	17.99
24	32.09	74.20	17.78
25	31.68	72.97	17.99
26	31.48	72.56	18.60
27	30.86	70.93	18.60
28	28.82	65.82	17.58
29	28.62	67.45	16.35
30	29.23	68.07	16.76

TABLE VII.- Continued

(c) $\Lambda = 10^0$

Thermocouple no.	h, $\text{W/m}^2\text{-K}$, at -		
	$M_\infty = 2.4$		$M_\infty = 4.5$ $R = 10 \times 10^6 \text{ per m}$
	$R = 3.3 \times 10^6 \text{ per m}$	$R = 10 \times 10^6 \text{ per m}$	
1	28.00	64.39	16.57
2	25.35	57.85	13.29
3	23.30	52.53	12.47
4	24.73	55.60	12.06
5	27.19	62.96	14.31
6	28.82	66.23	15.74
7	30.05	69.50	15.13
8	30.46	71.54	15.94
9	31.27	72.97	18.19
10	32.09	74.40	18.40
11	33.32	75.42	21.26
12	31.89	72.77	21.26
13	30.25	67.45	19.42
14	28.62	55.02	19.01
15	28.21	65.11	17.78
16	27.59	63.77	16.76
17	25.14	56.41	13.29
18	23.10	52.53	13.29
19	24.53	55.60	12.67
20	26.78	61.93	14.31
21	28.21	65.20	16.15
22	29.64	70.11	16.15
23	30.86	73.18	16.35
24	31.89	75.83	17.99
25	32.91	78.08	19.62
26	33.52	79.10	22.28
27	33.73	78.29	22.89
28	30.86	70.72	21.26
29	28.62	68.68	19.21
30	27.39	64.18	17.99

TABLE VII.- Continued

(d) $\Lambda = 15^\circ$

Thermocouple no.	$h, \text{W/m}^2\text{-K, at -}$		
	$M_\infty = 2.4$		$M_\infty = 4.5$ $R = 10 \times 10^6 \text{ per m}$
	$R = 3.3 \times 10^6 \text{ per m}$	$R = 10 \times 10^6 \text{ per m}$	
1	28.41	68.68	15.94
2	24.73	58.87	12.67
3	21.46	49.46	13.08
4	22.89	49.87	12.67
5	26.78	61.16	13.49
6	28.62	69.50	13.69
7	29.23	76.04	12.47
8	30.46	79.10	13.49
9	32.50	82.37	19.01
10	34.34	84.62	22.08
11	36.59	85.85	24.73
12	35.57	83.80	23.91
13	33.11	75.83	20.03
14	30.25	72.97	19.62
15	26.62	69.29	17.17
16	26.98	66.43	15.53
17	24.12	56.01	13.49
18	21.26	49.26	13.90
19	22.48	49.87	13.49
20	26.98	60.71	13.69
21	29.02	70.72	14.92
22	29.84	77.88	13.29
23	30.25	81.15	15.13
24	32.30	84.01	19.62
25	34.54	87.07	23.10
26	36.59	89.12	26.16
27	36.79	88.91	24.53
28	32.91	78.69	21.67
29	29.43	73.58	20.44
30	26.78	67.45	17.58

TABLE VII.- Continued

(e) $\Lambda = 20^\circ$

Thermocouple no.	h, $\text{W/m}^2\text{-K}$, at -		
	$M_\infty = 2.4$		$M_\infty = 4.5$ $R = 10 \times 10^6 \text{ per m}$
	$R = 3.3 \times 10^6 \text{ per m}$	$R = 10 \times 10^6 \text{ per m}$	
1	30.25	74.61	15.53
2	25.96	64.79	13.69
3	23.91	55.60	15.13
4	23.71	49.87	15.13
5	27.59	59.28	14.10
6	28.41	72.36	14.31
7	26.98	79.72	12.67
8	30.05	79.92	17.78
9	33.93	84.42	24.53
10	37.20	88.51	28.82
11	40.27	92.39	29.43
12	39.24	90.34	26.16
13	35.16	82.58	20.64
14	33.11	78.49	21.05
15	30.25	73.38	17.37
16	28.82	69.50	15.33
17	24.94	58.25	14.72
18	22.69	53.55	15.53
19	23.30	48.85	15.13
20	27.80	59.68	14.92
21	29.02	75.22	14.92
22	26.37	82.37	13.69
23	29.64	83.40	18.80
24	34.13	86.87	25.55
25	37.61	91.98	29.43
26	40.88	96.68	31.89
27	40.06	96.89	27.39
28	34.75	85.23	21.26
29	31.48	80.12	20.03
30	28.62	75.83	17.58

TABLE VII.- Continued

(f) $\Lambda = 30^\circ$

Thermocouple no.	h, $\text{W/m}^2\text{-K}$, at -		
	$M_\infty = 2.4$		$M_\infty = 4,5$ $R = 10 \times 10^6 \text{ per m}$
	$R = 3.3 \times 10^6 \text{ per m}$	$R = 10 \times 10^6 \text{ per m}$	
1	32.91	75.01	15.33
2	30.46	67.04	14.10
3	29.43	66.63	14.72
4	29.84	65.82	14.10
5	32.09	65.61	16.97
6	32.70	78.08	14.72
7	29.23	83.60	15.74
8	35.97	82.58	23.51
9	43.13	94.64	30.46
10	48.03	104.86	31.68
11	49.87	107.92	31.07
12	45.79	100.16	26.57
13	38.43	86.67	21.05
14	37.41	83.60	20.64
15	32.09	73.79	15.94
16	31.07	69.70	15.74
17	28.41	62.14	15.33
18	27.80	62.55	15.13
19	28.20	60.91	14.72
20	30.46	62.55	16.56
21	31.89	77.26	15.94
22	29.23	83.40	16.97
23	34.34	82.58	23.71
24	40.68	93.62	28.41
25	44.56	98.93	30.66
26	45.79	102.40	31.48
27	42.11	95.45	27.59
28	35.16	81.15	21.05
29	32.09	75.42	19.01
30	30.86	69.70	17.78

TABLE VII.- Continued

(g) $\Lambda = 45^\circ$

Thermocouple no.	h, $\text{W/m}^2\text{-K}$, at -		
	$M_\infty = 2.4$		$M_\infty = 4.5$ $R = 10 \times 10^6 \text{ per m}$
	$R = 3.3 \times 10^6 \text{ per m}$	$R = 10 \times 10^6 \text{ per m}$	
1	37.41	80.12	17.58
2	31.68	71.13	12.88
3	29.02	65.41	13.49
4	28.21	64.79	13.08
5	30.86	71.54	12.67
6	29.84	78.90	9.20
7	23.91	65.20	12.88
8	37.61	85.23	23.71
9	45.99	97.91	29.64
10	50.90	106.70	34.34
11	53.76	110.58	35.57
12	50.90	106.29	31.27
13	44.15	96.89	23.91
14	41.29	91.57	23.51
15	35.57	82.78	19.62
16	33.73	78.08	16.76
17	29.43	68.68	13.49
18	27.19	64.18	14.51
19	26.98	62.55	12.88
20	28.82	68.06	12.06
21	28.00	75.63	9.40
22	23.10	63.36	13.08
23	34.54	80.33	23.10
24	43.54	95.05	30.25
25	48.65	102.61	34.34
26	51.51	107.11	36.38
27	50.90	106.08	33.11
28	42.92	94.43	25.75
29	38.43	85.03	22.89
30	35.36	77.06	18.60

TABLE VII.- Continued

(h) $\Lambda = 60^\circ$

Thermocouple no.	h, $\text{W/m}^2\text{-K}$, at -		
	$M_\infty = 2.4$		$M_\infty = 4.5$ $R = 10 \times 10^6 \text{ per m}$
	$R = 3.3 \times 10^6 \text{ per m}$	$R = 10 \times 10^6 \text{ per m}$	
1	35.77	87.69	17.17
2	29.64	77.06	13.08
3	28.62	70.31	12.26
4	28.62	68.68	12.06
5	31.68	74.81	11.86
6	28.82	69.31	9.20
7	24.12	63.98	13.08
8	38.84	85.85	23.71
9	49.46	103.63	30.05
10	56.21	116.10	34.75
11	60.09	123.46	36.79
12	56.01	118.76	32.70
13	47.01	105.47	24.73
14	44.15	100.56	23.71
15	37.20	89.53	18.60
16	33.73	84.42	16.15
17	28.21	73.38	12.88
18	27.80	68.68	12.06
19	27.39	65.20	11.65
20	29.84	72.15	11.04
21	26.98	76.30	8.18
22	25.53	64.79	15.53
23	38.63	86.05	24.12
24	48.85	103.43	31.89
25	54.98	114.05	36.59
26	58.46	121.82	39.65
27	55.19	119.17	35.16
28	44.15	101.59	26.78
29	39.04	90.55	21.67
30	33.52	81.35	17.99

TABLE VII.- Concluded

(i) $\Lambda = 90^\circ$

Thermocouple no.	$h, \text{ W/m}^2\text{-K, at -}$		
	$M_\infty = 2.4$		$M_\infty = 4.5$ $R = 10 \times 10^6 \text{ per m}$
	$R = 3.3 \times 10^6 \text{ per m}$	$R = 10 \times 10^6 \text{ per m}$	
1	39.86	93.21	21.05
2	32.30	80.53	15.74
3	28.82	71.54	14.31
4	28.41	68.47	13.49
5	31.89	77.67	12.67
6	27.39	78.90	10.63
7	24.53	63.16	15.53
8	41.70	90.34	26.57
9	52.33	107.11	34.54
10	60.09	123.05	39.86
11	65.41	134.70	43.74
12	61.93	131.22	39.24
13	52.33	115.89	30.46
14	48.44	107.72	28.00
15	41.49	95.25	22.48
16	38.63	89.94	20.44
17	31.68	75.83	16.56
18	29.02	70.52	14.10
19	27.59	65.41	13.29
20	29.84	73.79	12.06
21	26.16	75.63	10.02
22	26.16	65.20	16.76
23	41.90	90.14	26.98
24	52.33	108.33	34.95
25	60.30	122.44	41.70
26	65.41	134.70	44.76
27	63.77	133.68	41.70
28	51.51	113.44	30.46
29	44.15	99.13	24.12
30	38.84	89.32	21.05

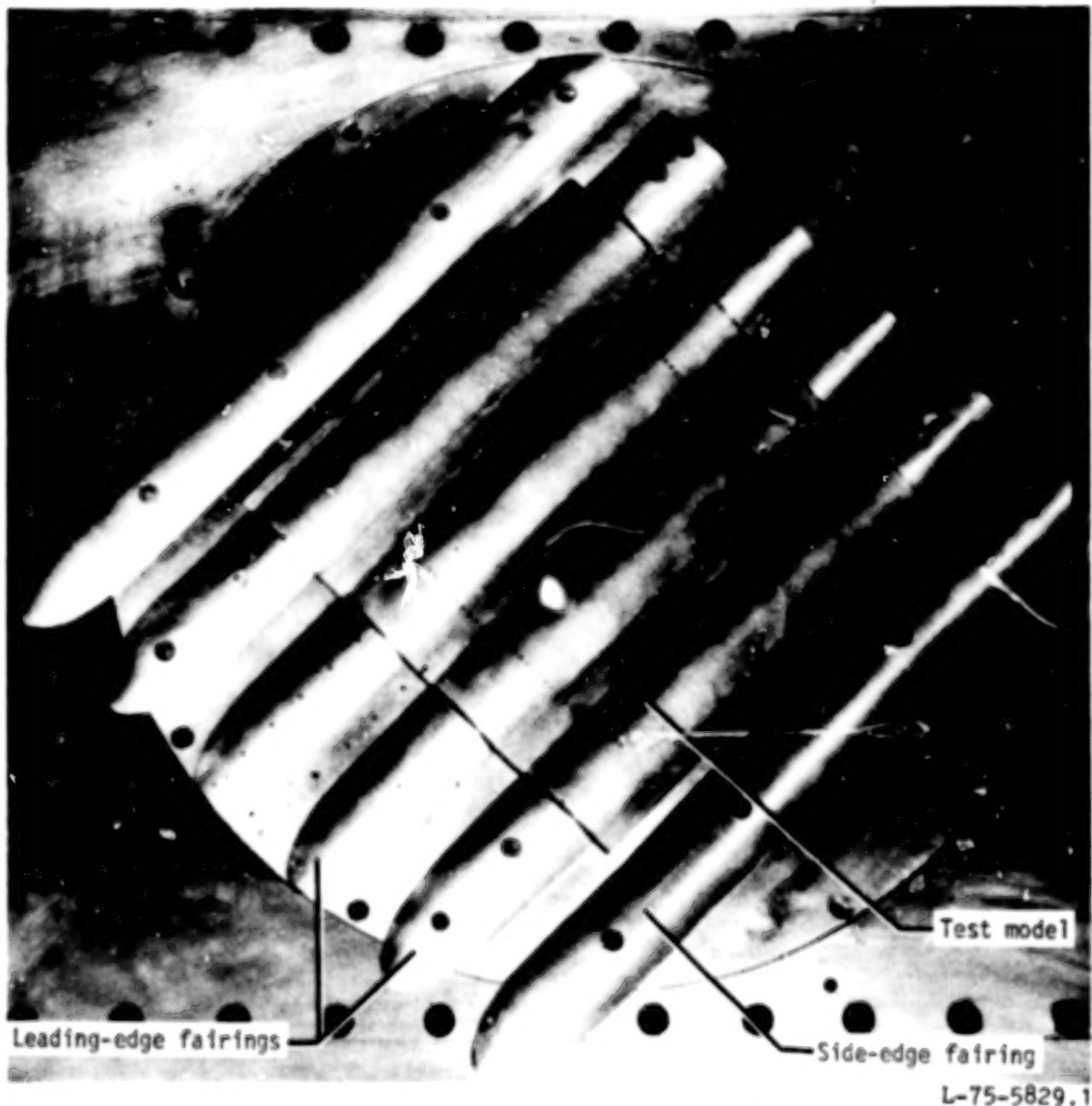


Figure 1.- Corrugated test panel mounted in circular plate.

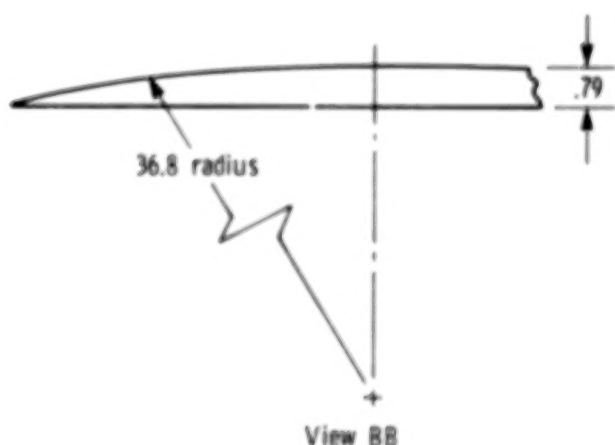
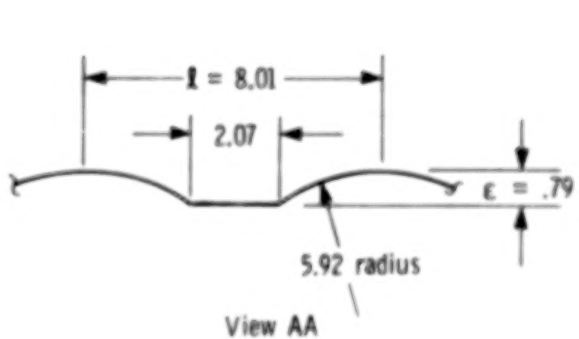
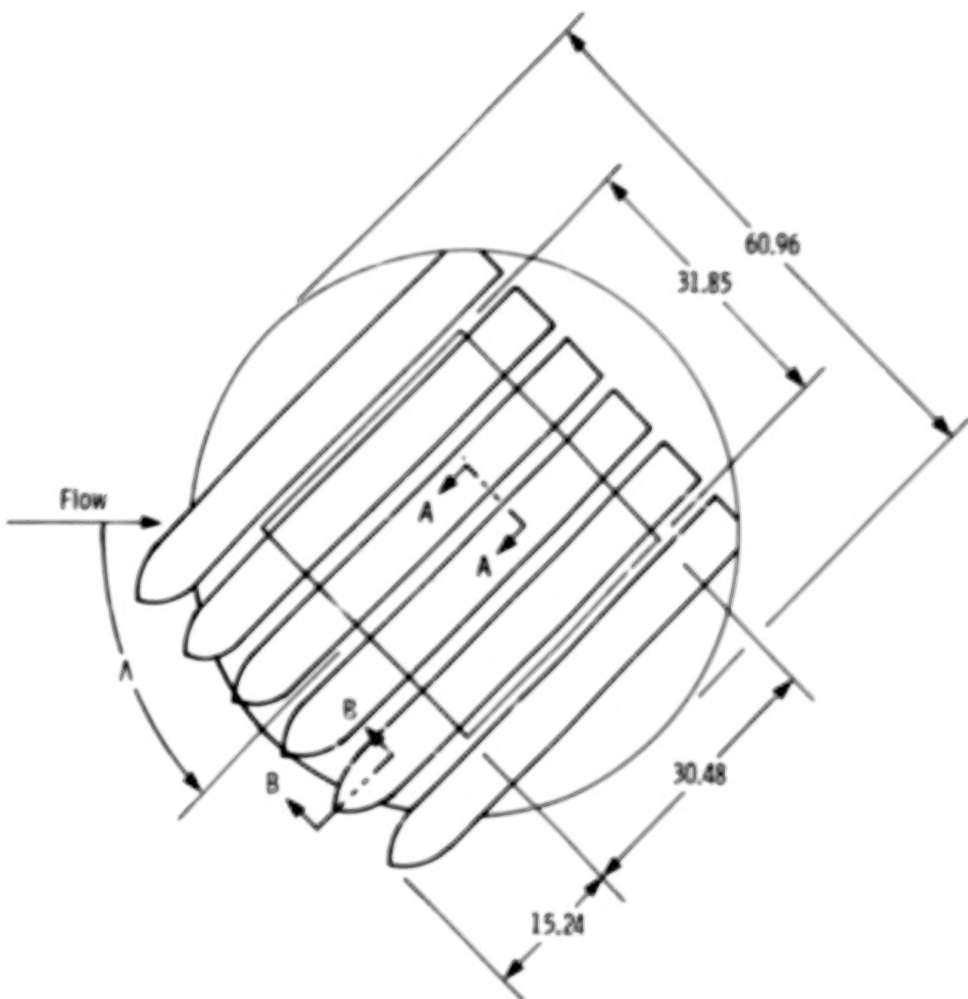


Figure 2.- Details of corrugated surface model. Dimensions are given in centimeters.

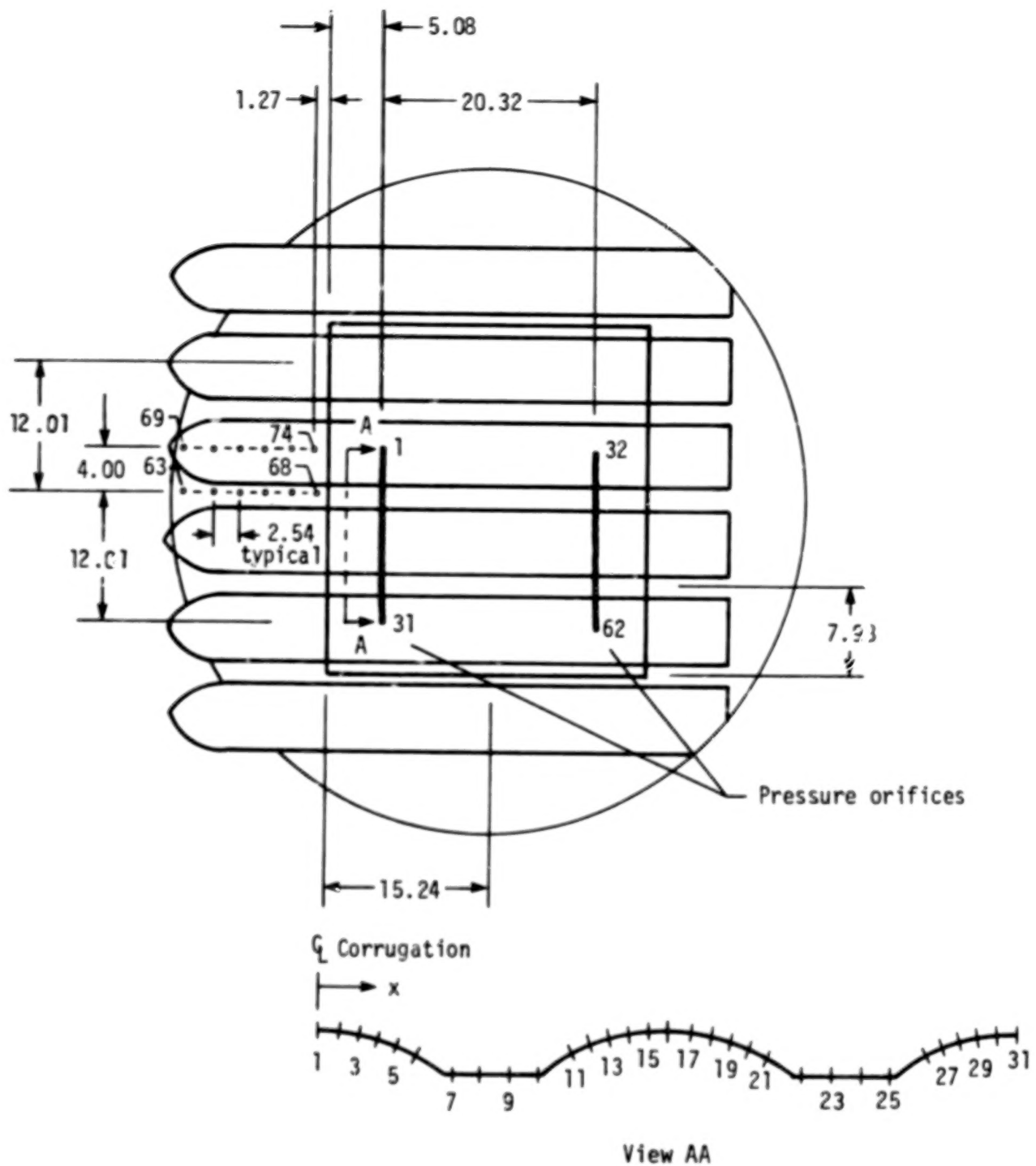


Figure 3.- Instrumentation for pressure model. Dimensions are given in centimeters.

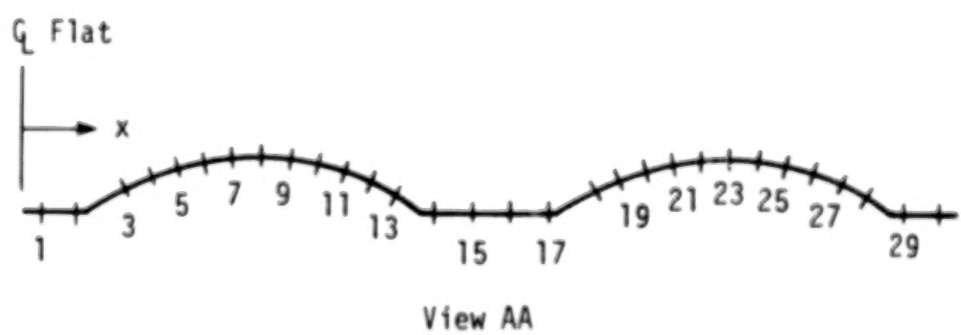
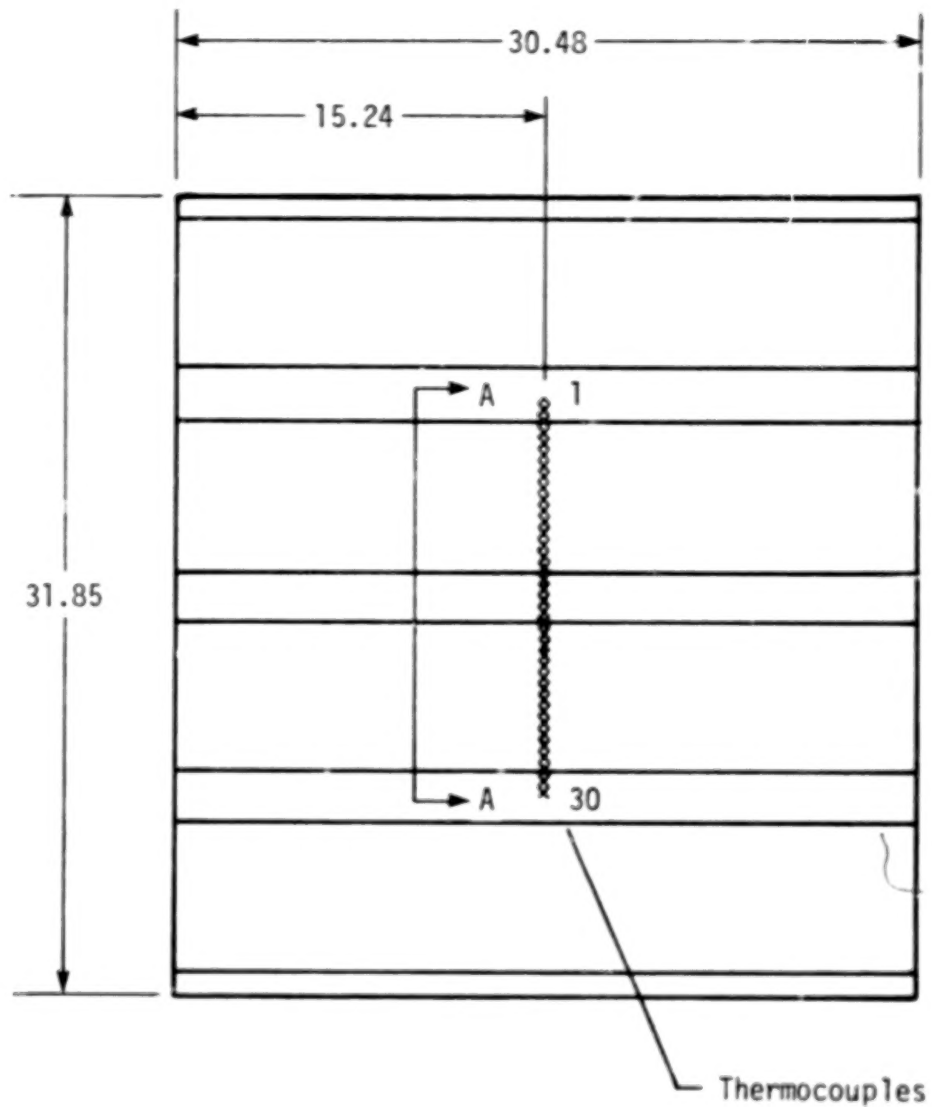


Figure 4.- Instrumentation for heat-transfer model. Dimensions are given in centimeters.

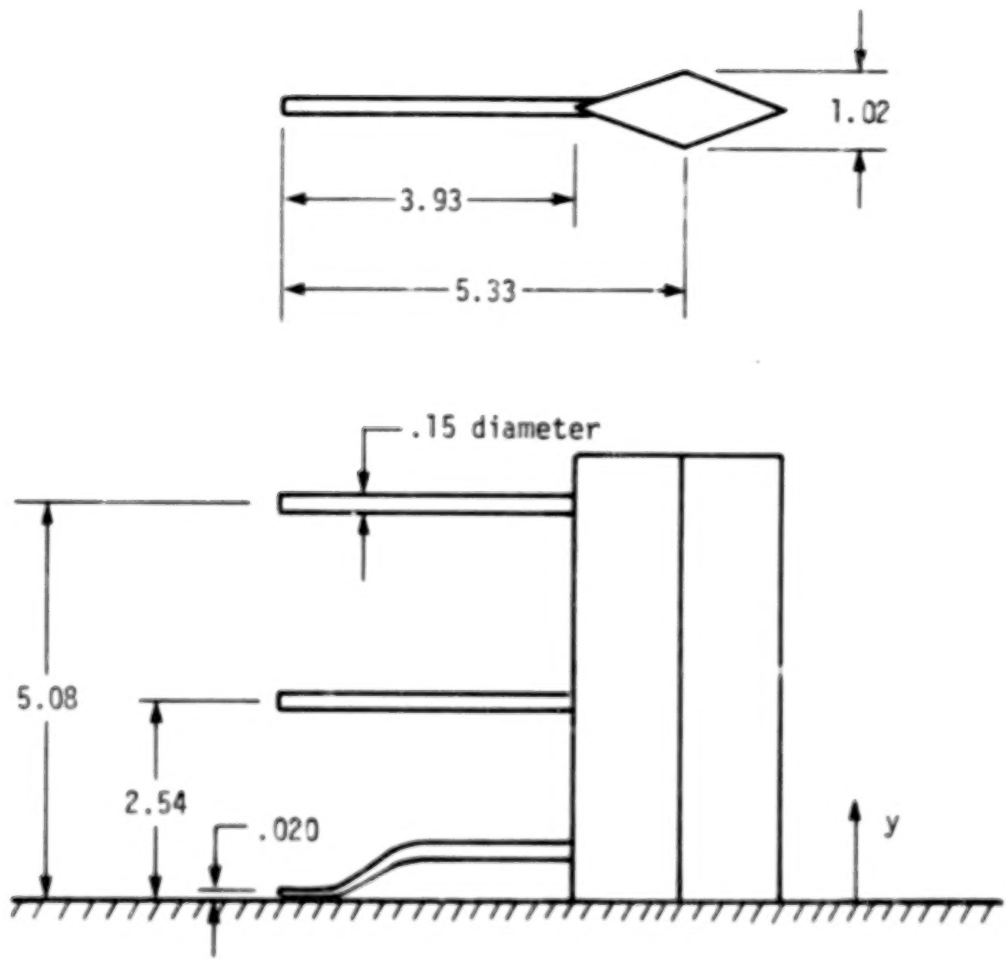


Figure 5.- Details of boundary-layer survey rake.

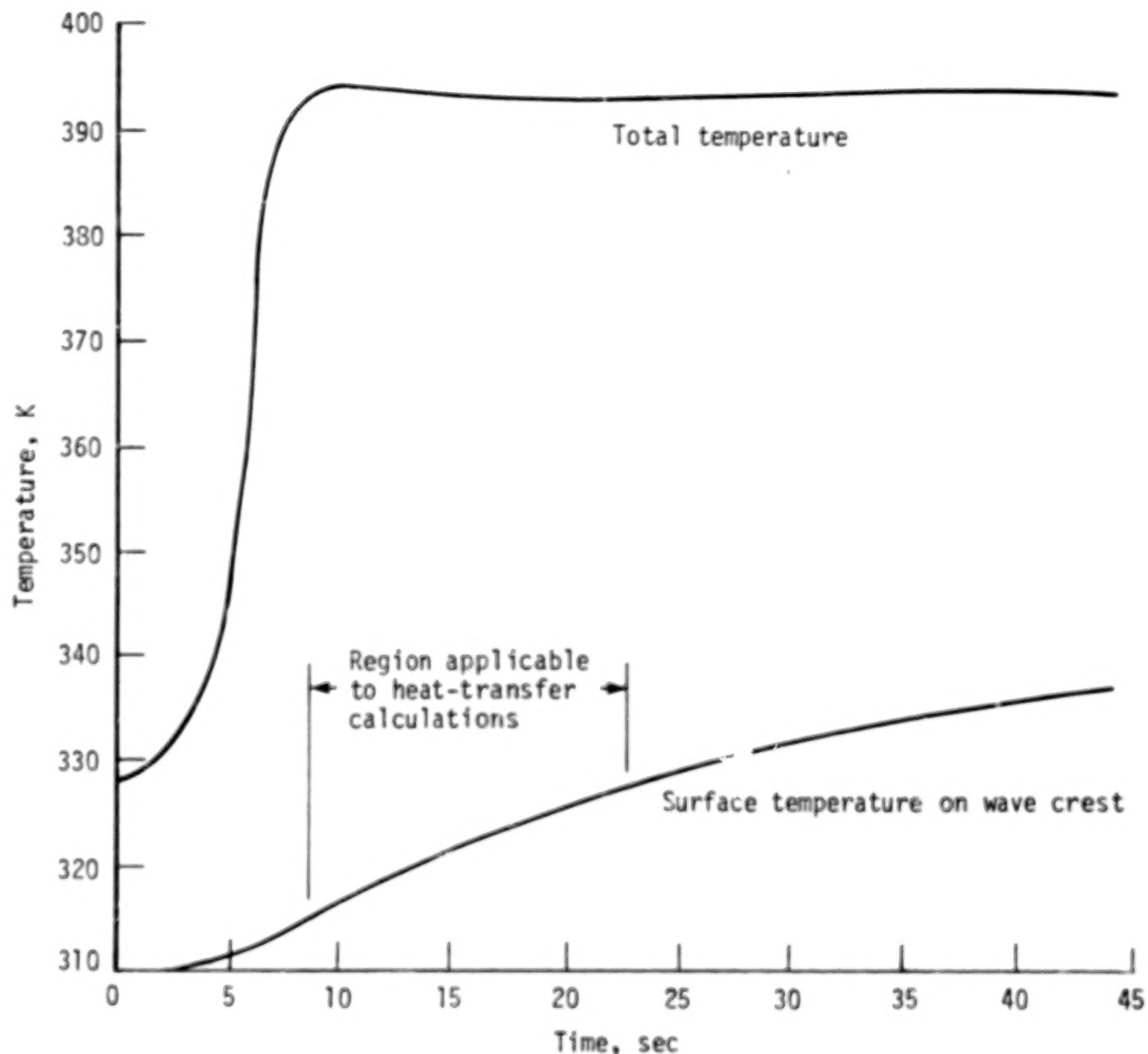


Figure 6.- Typical total and surface temperature histories for heat-transfer tests.

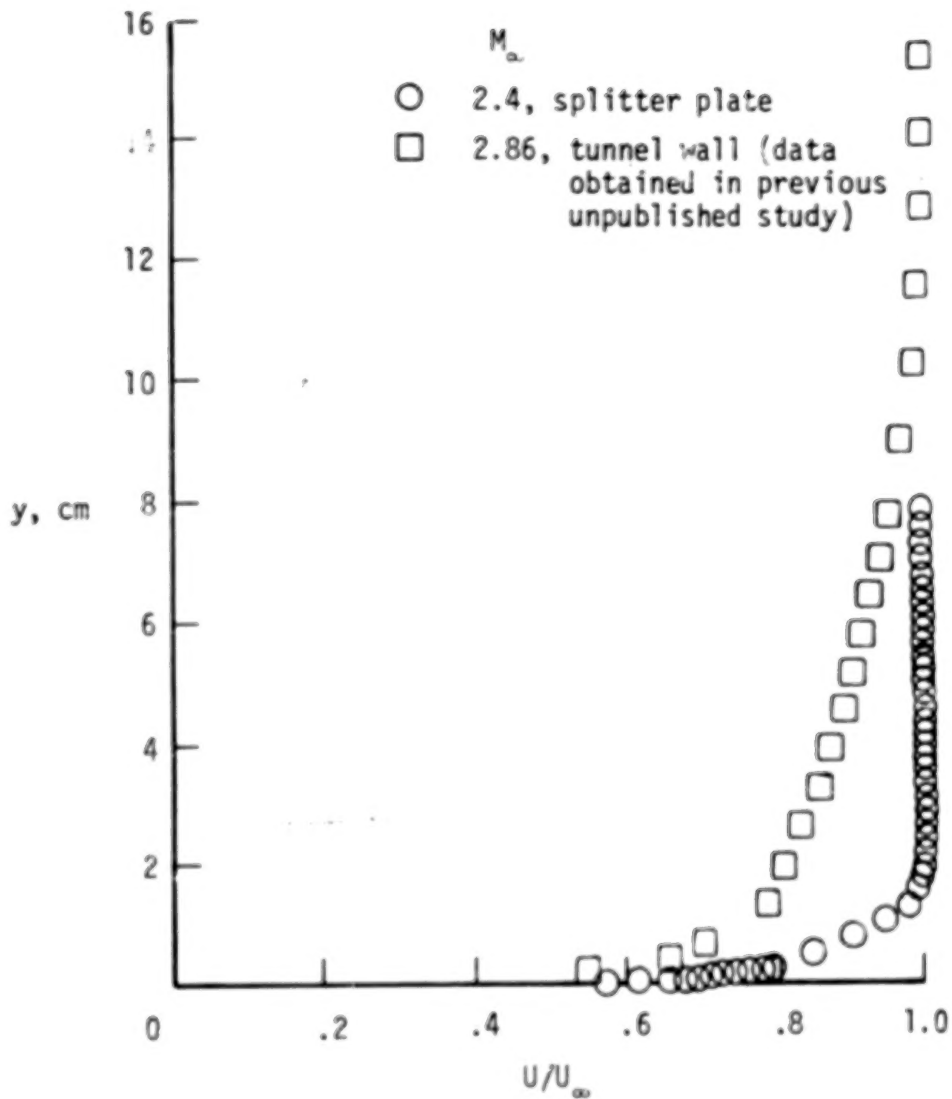
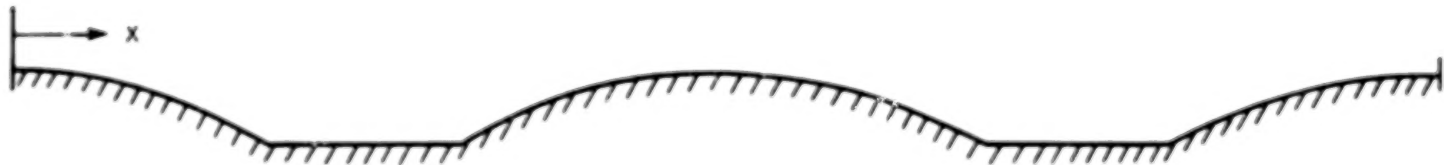
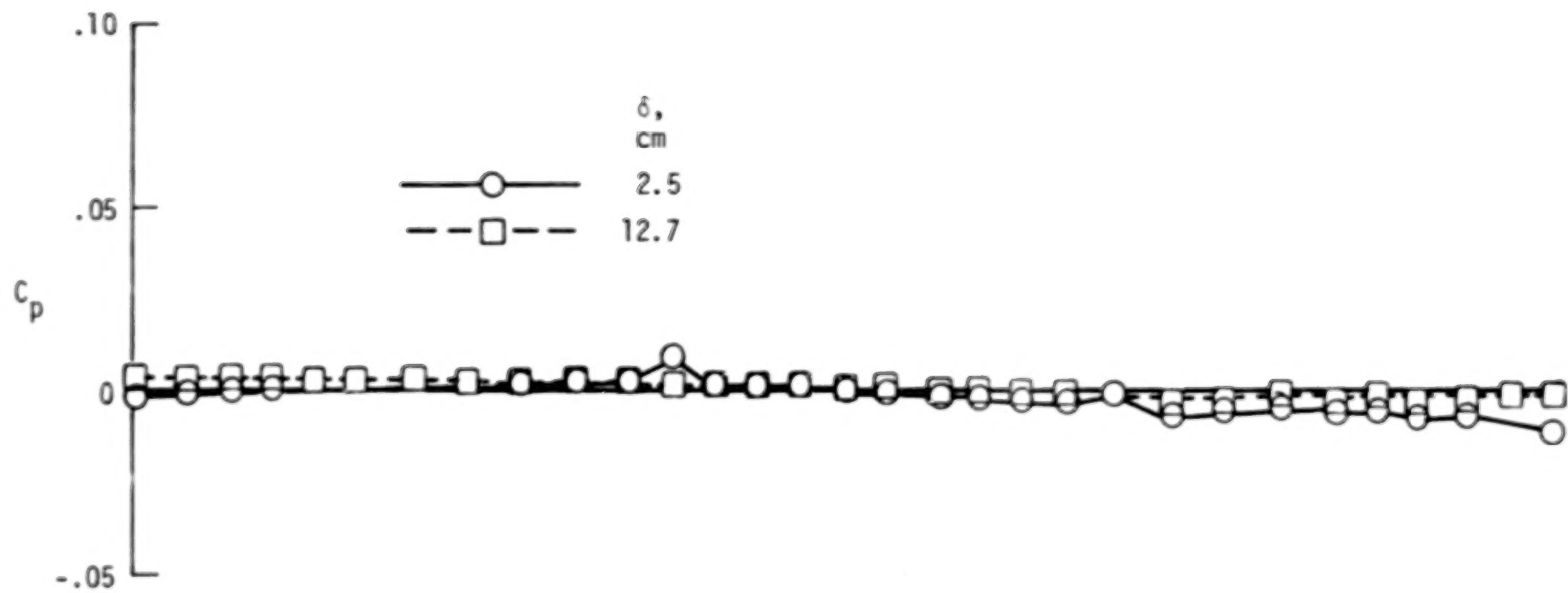


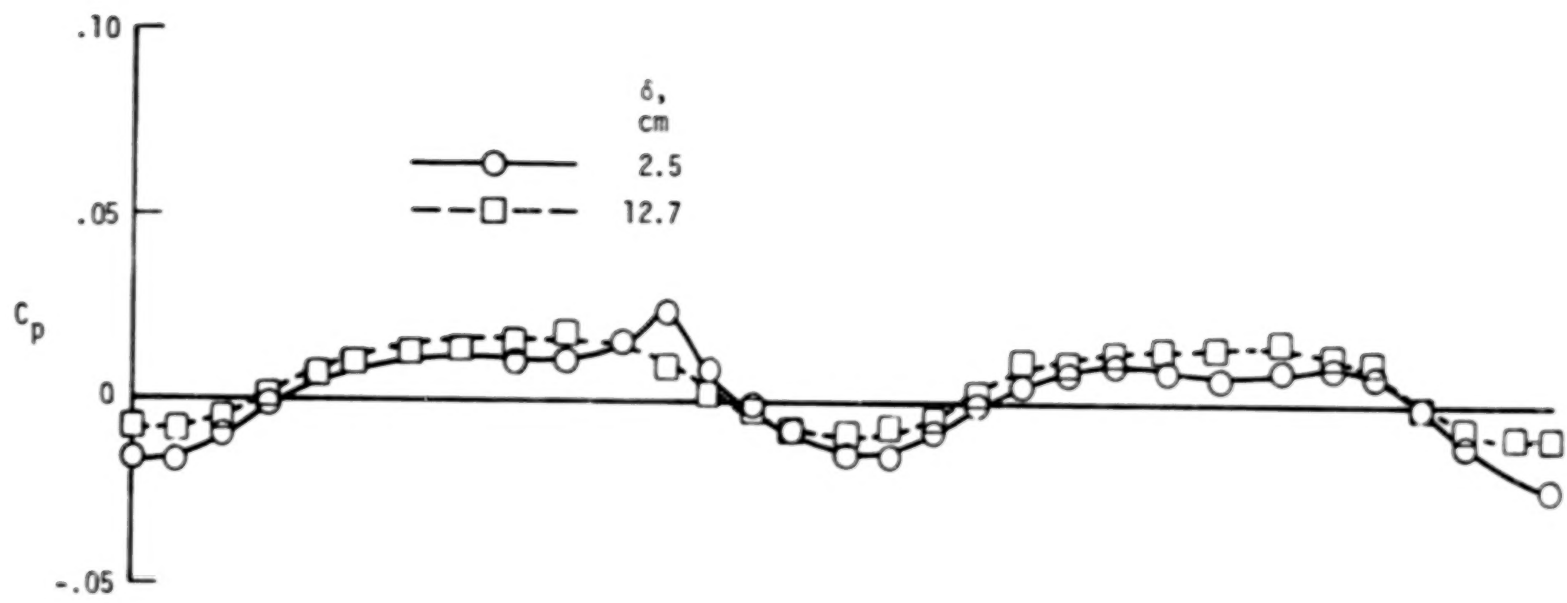
Figure 7.- typical boundary-layer velocity distributions on flat surface in splitter plate and tunnel wall for $R = 10 \times 10^6$ per meter.



(a) $\Lambda = 0^\circ$.

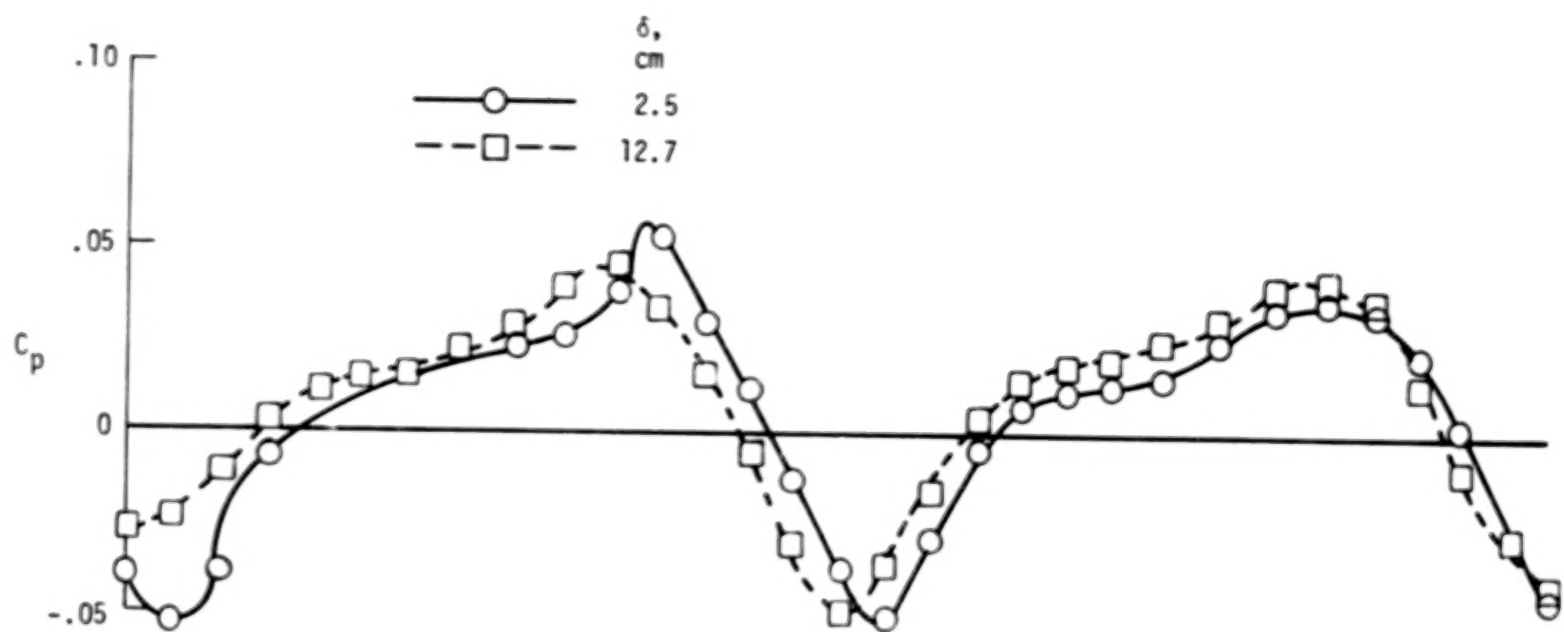
Figure 8.- Effect of boundary-layer thickness on pressure distributions over corrugated surface.
 $R = 10 \times 10^6$ per meter; $M_\infty = 2.4$. Table I gives pressure orifice x -locations.

60



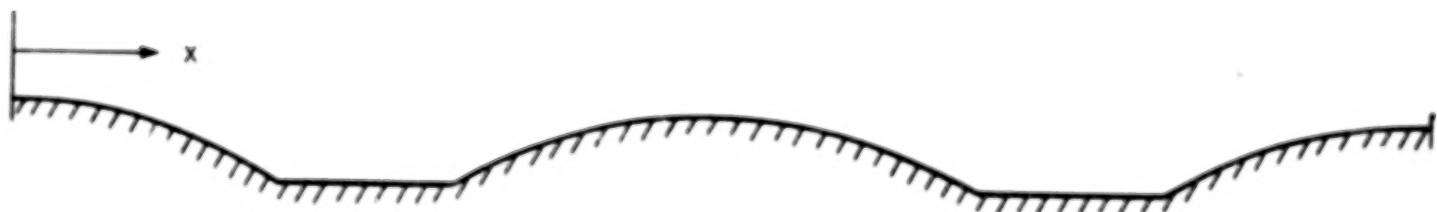
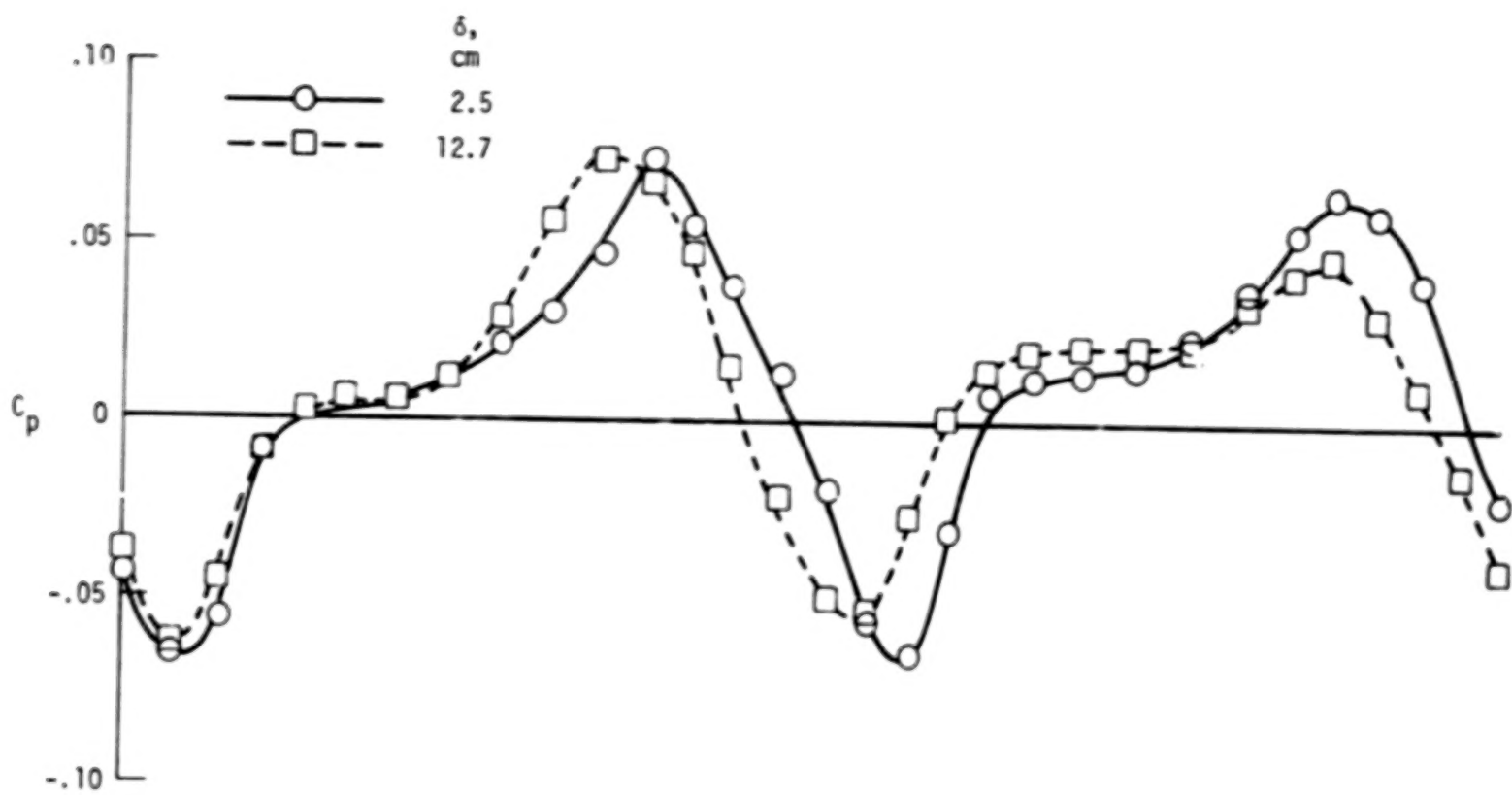
(b) $\Lambda = 15^\circ$.

Figure 8.- Continued.



(c) $\Lambda = 30^\circ$.

Figure 8.- Continued.



(d) $\Lambda = 45^\circ$.

Figure 8.- Concluded.

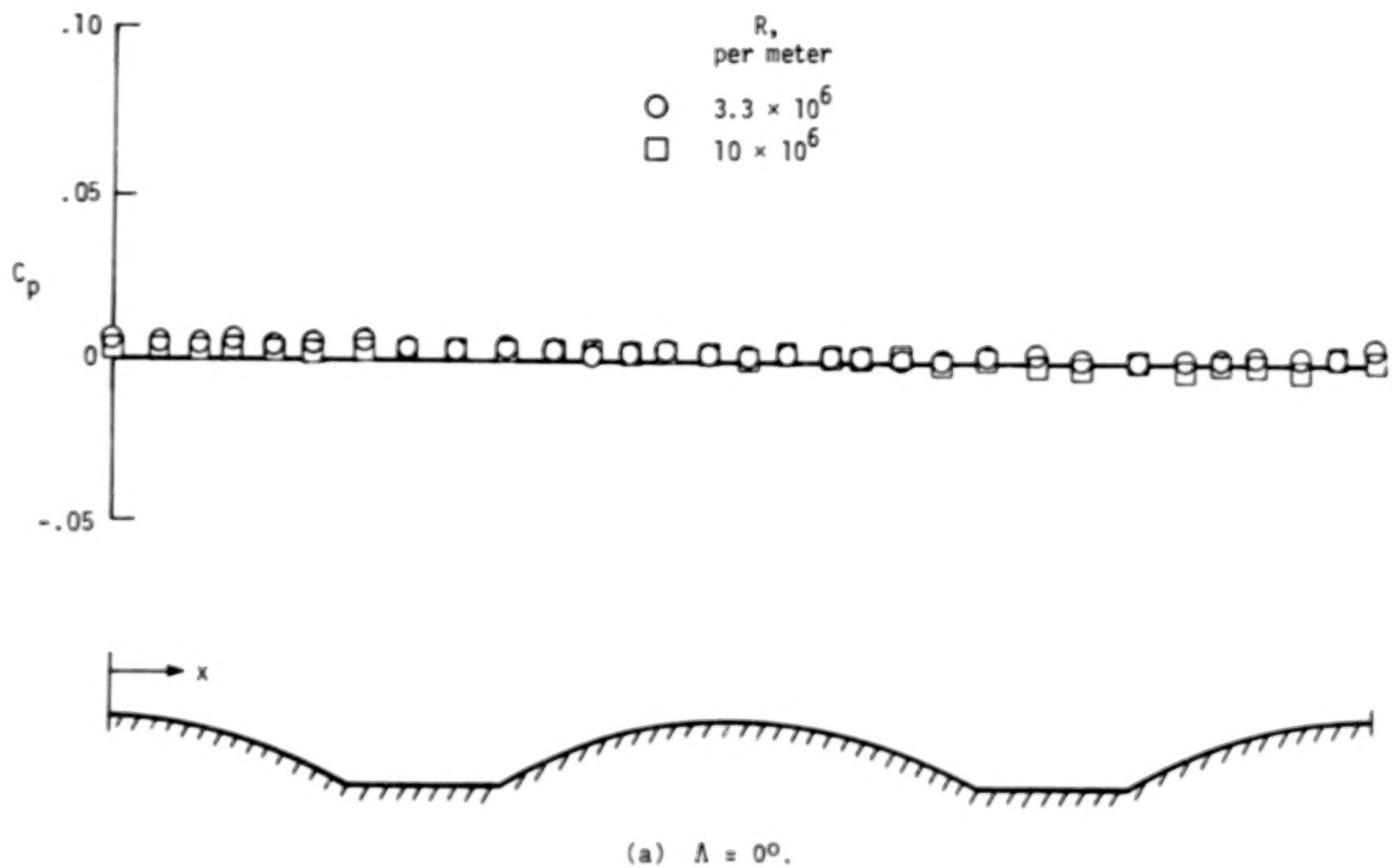
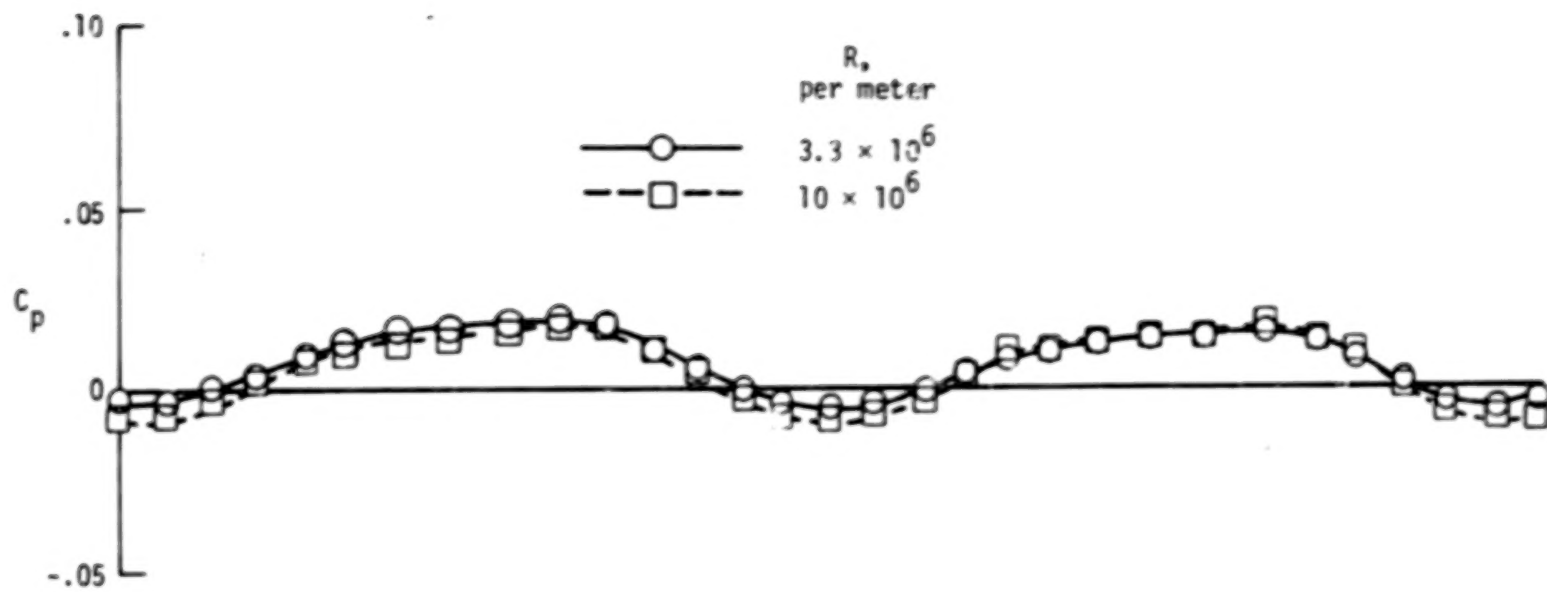
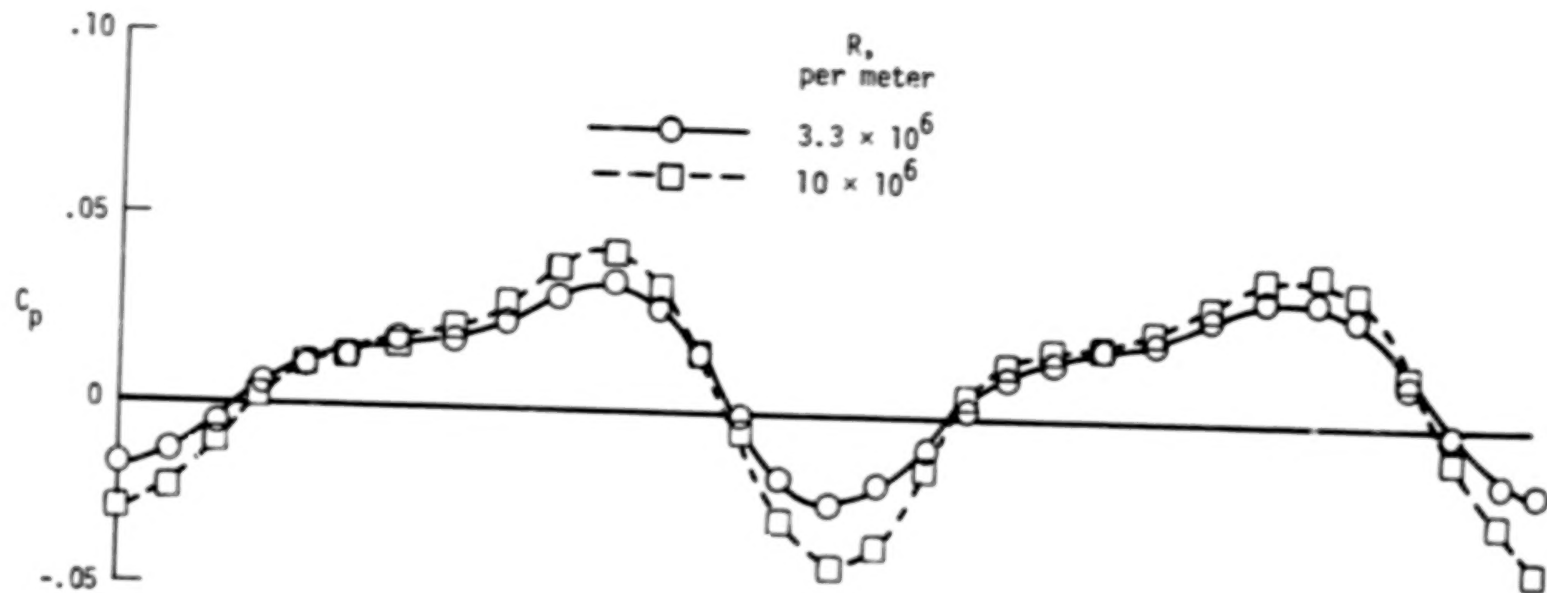


Figure 9.- Effects of Reynolds number on pressure distributions over corrugated surface.
 $\delta = 12.7 \text{ cm}$; $M_\infty = 2.4$. Table I gives pressure orifice x-locations.



(b) $\Lambda = 15^\circ$.

Figure 9.- Continued.



(c) $\lambda = 300$.

Figure 9.- Continued.

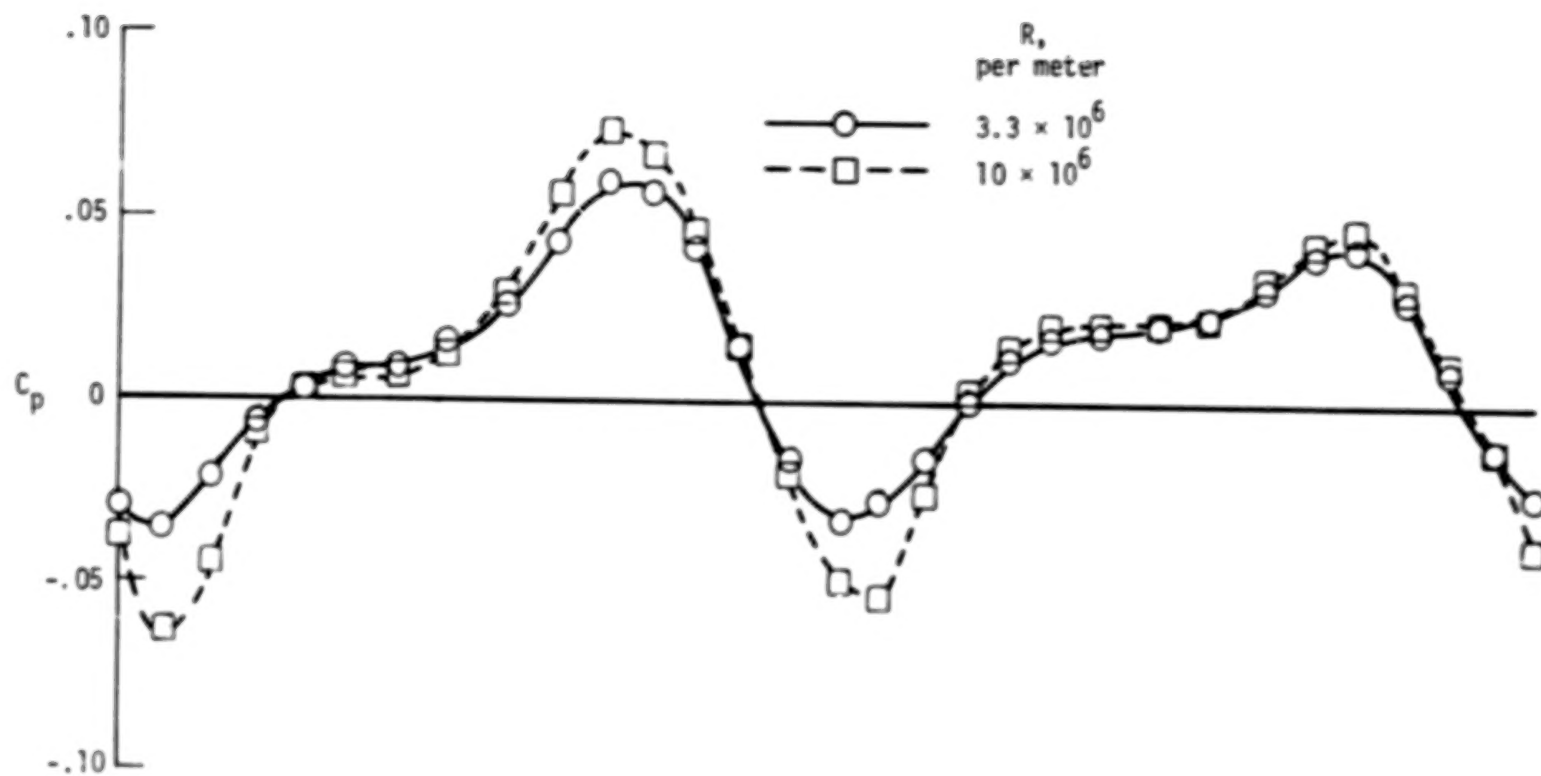
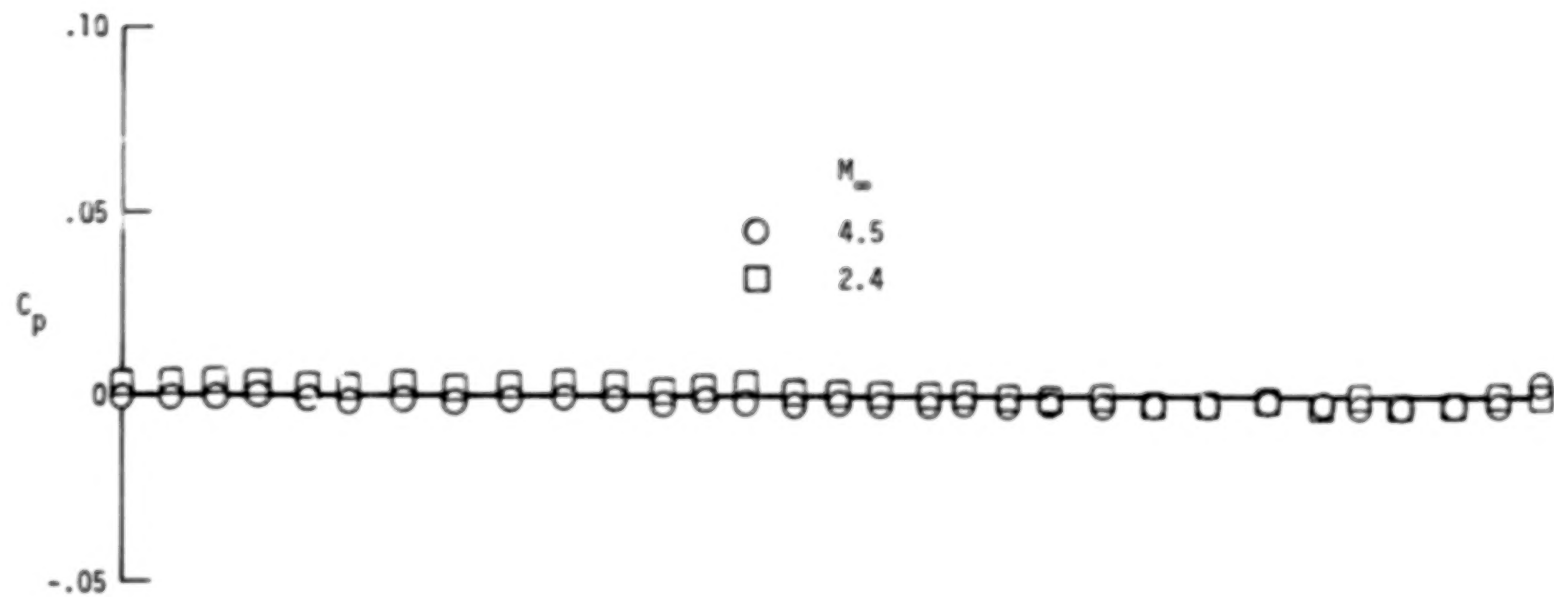
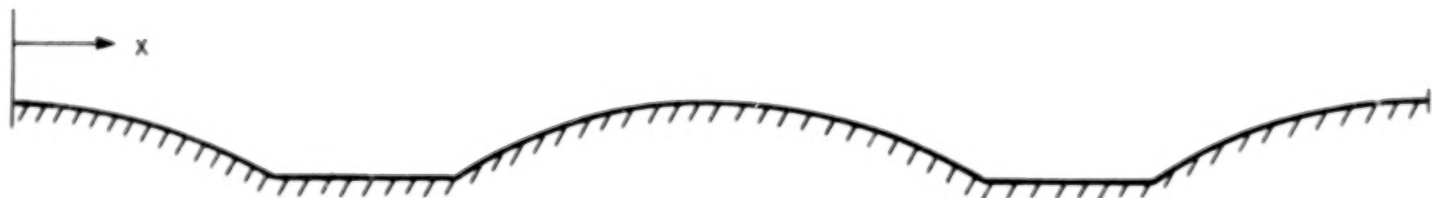
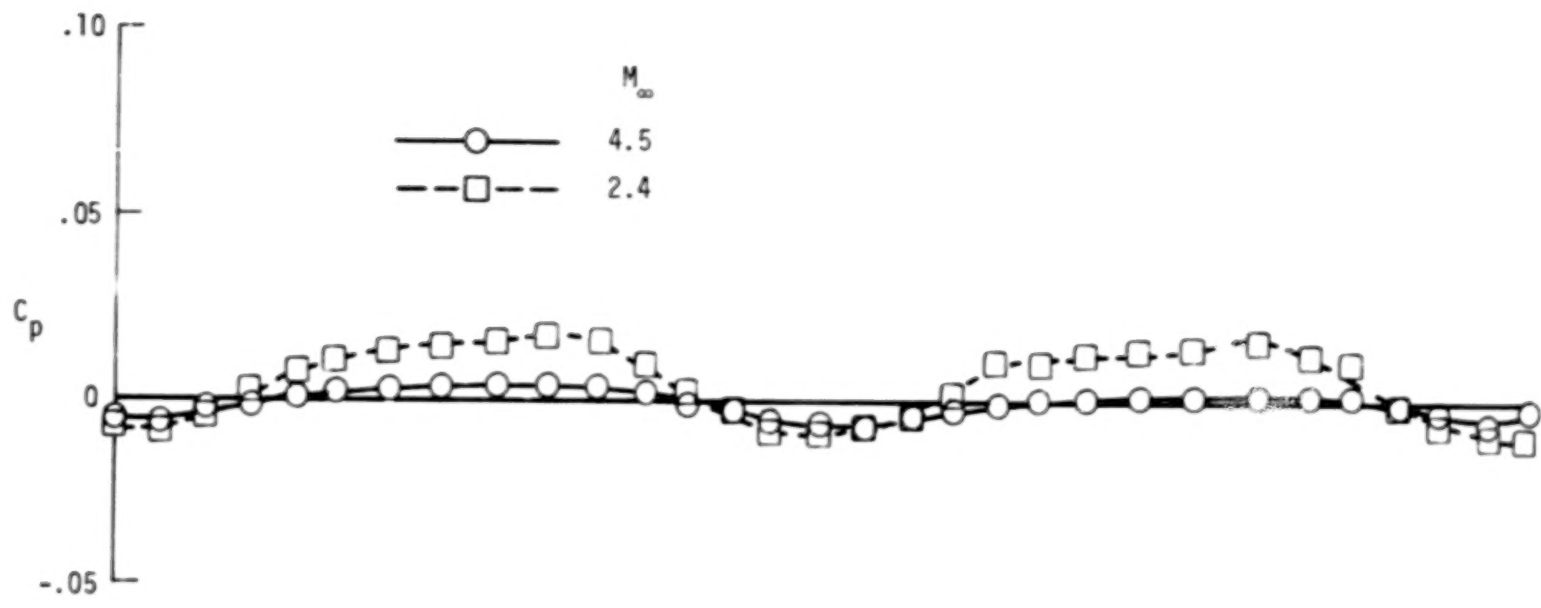


Figure 9.- Concluded.



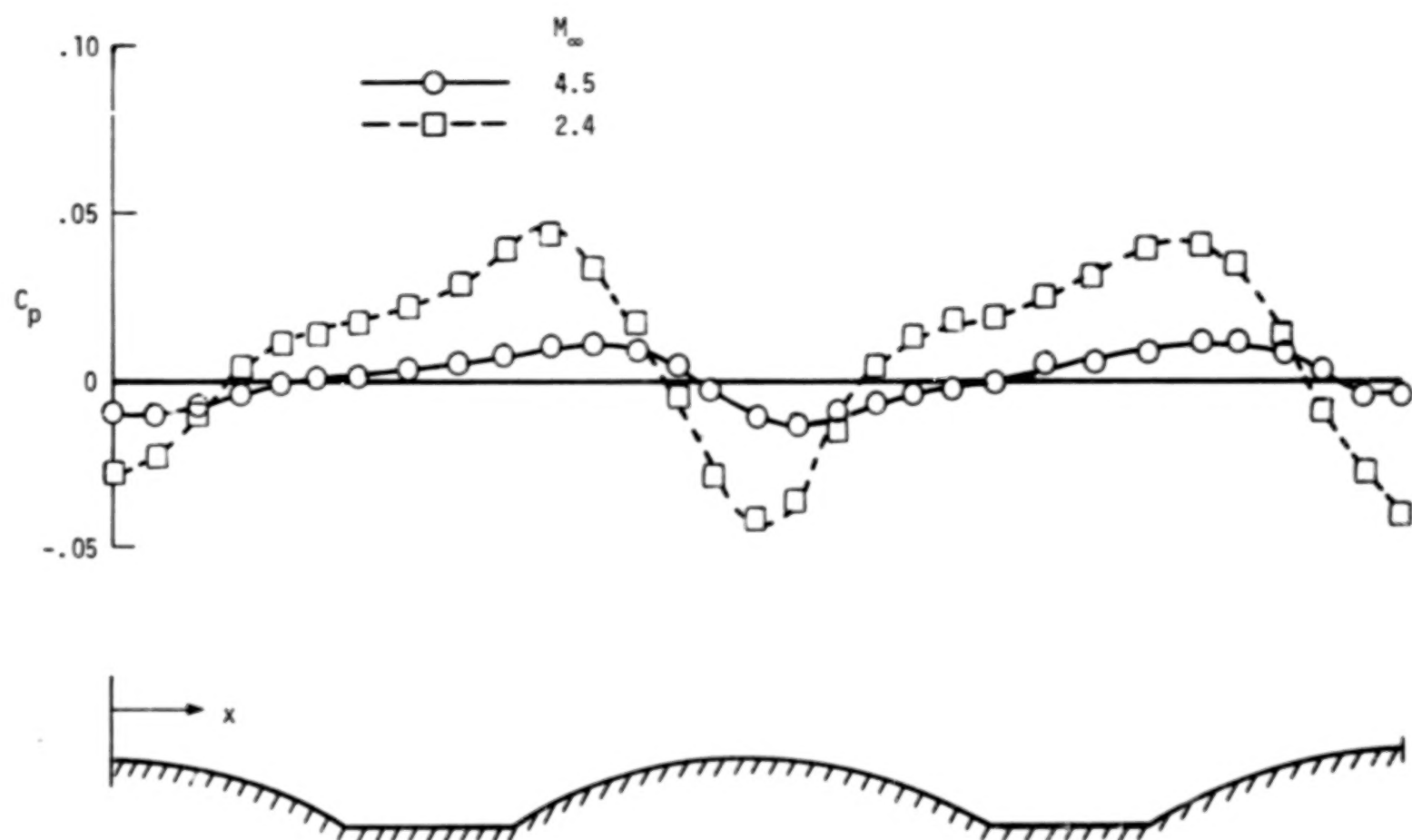
(a) $\Lambda = 0^\circ$.

Figure 10.- Effects of Mach number on pressure distributions over corrugated surface.
 $\delta = 12.7$ cm; $R = 10 \times 10^6$ per meter. Table I gives pressure orifice x -locations.



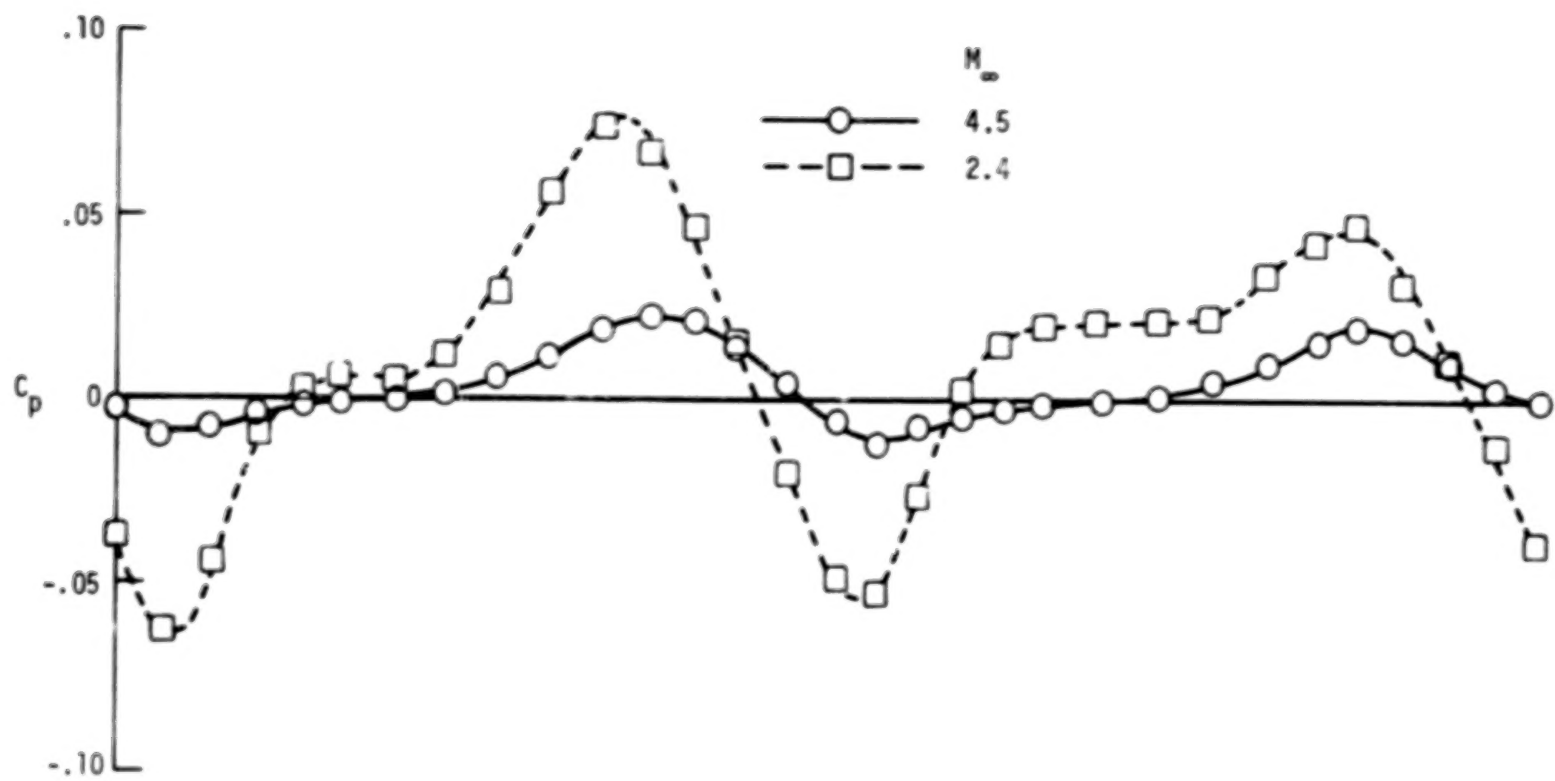
(b) $\Lambda = 15^\circ$.

Figure 10.- Continued.



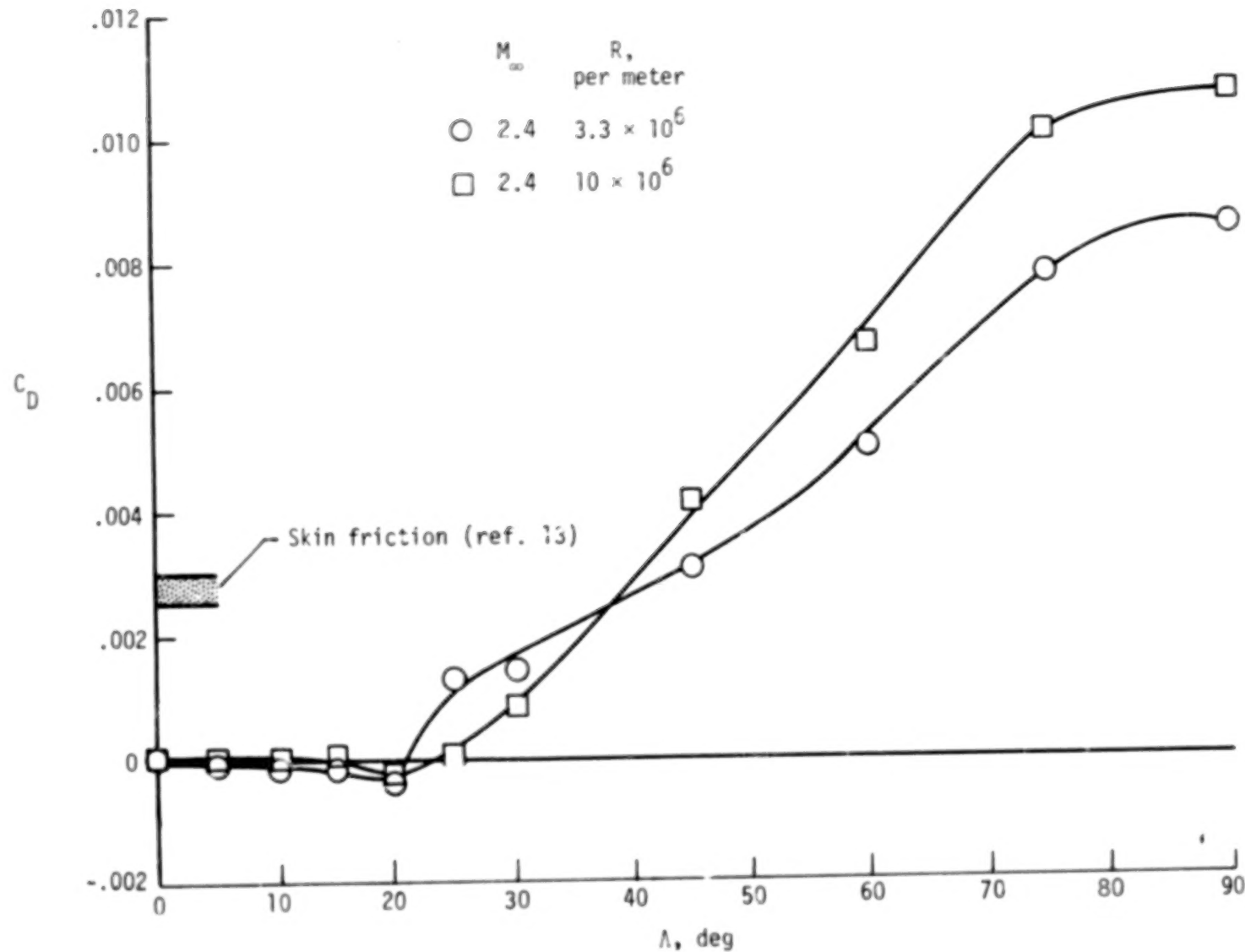
(c) $\Lambda = 30^\circ$.

Figure 10.- Continued.



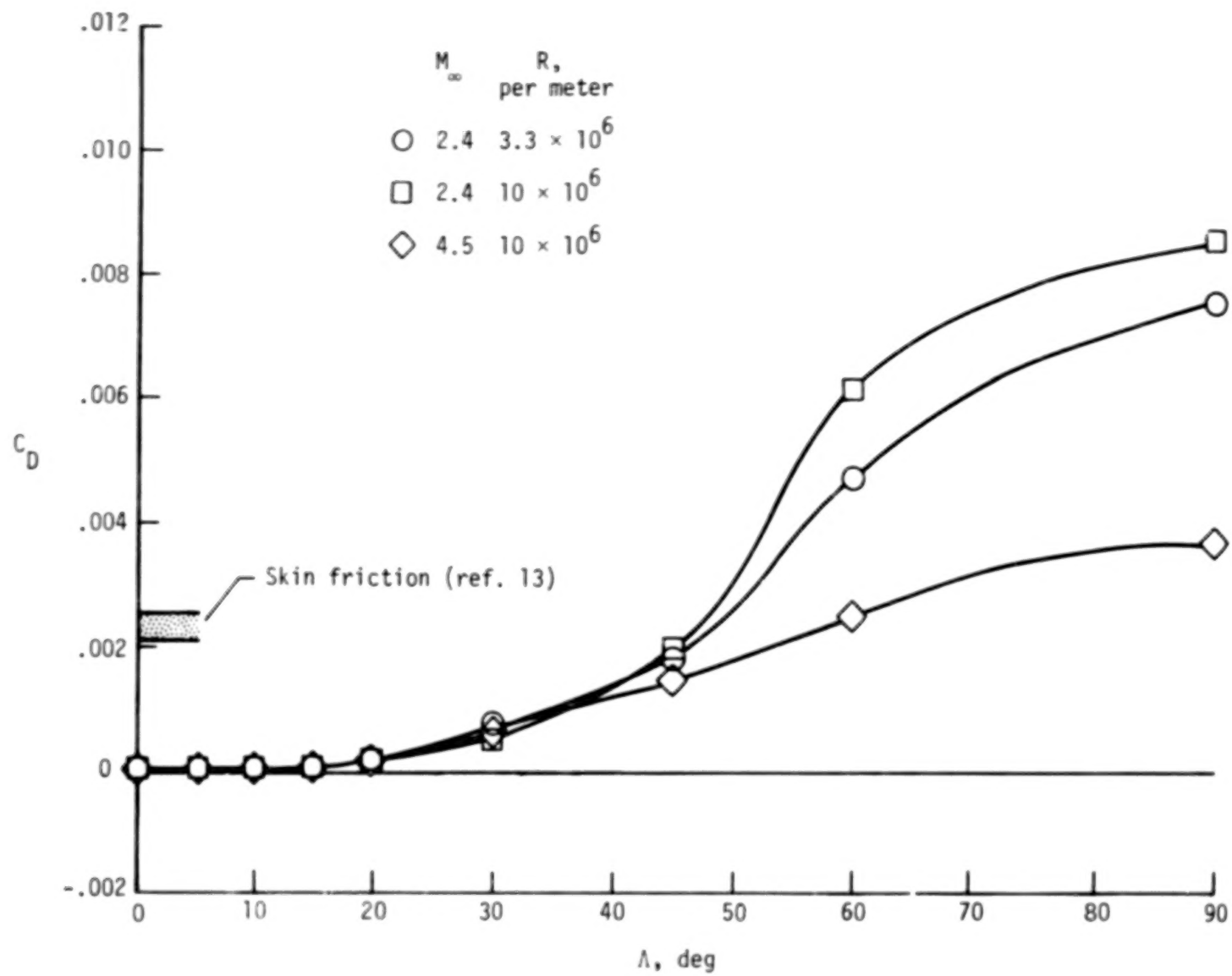
(d) $\Lambda = 45^\circ$.

Figure 10.- Concluded.



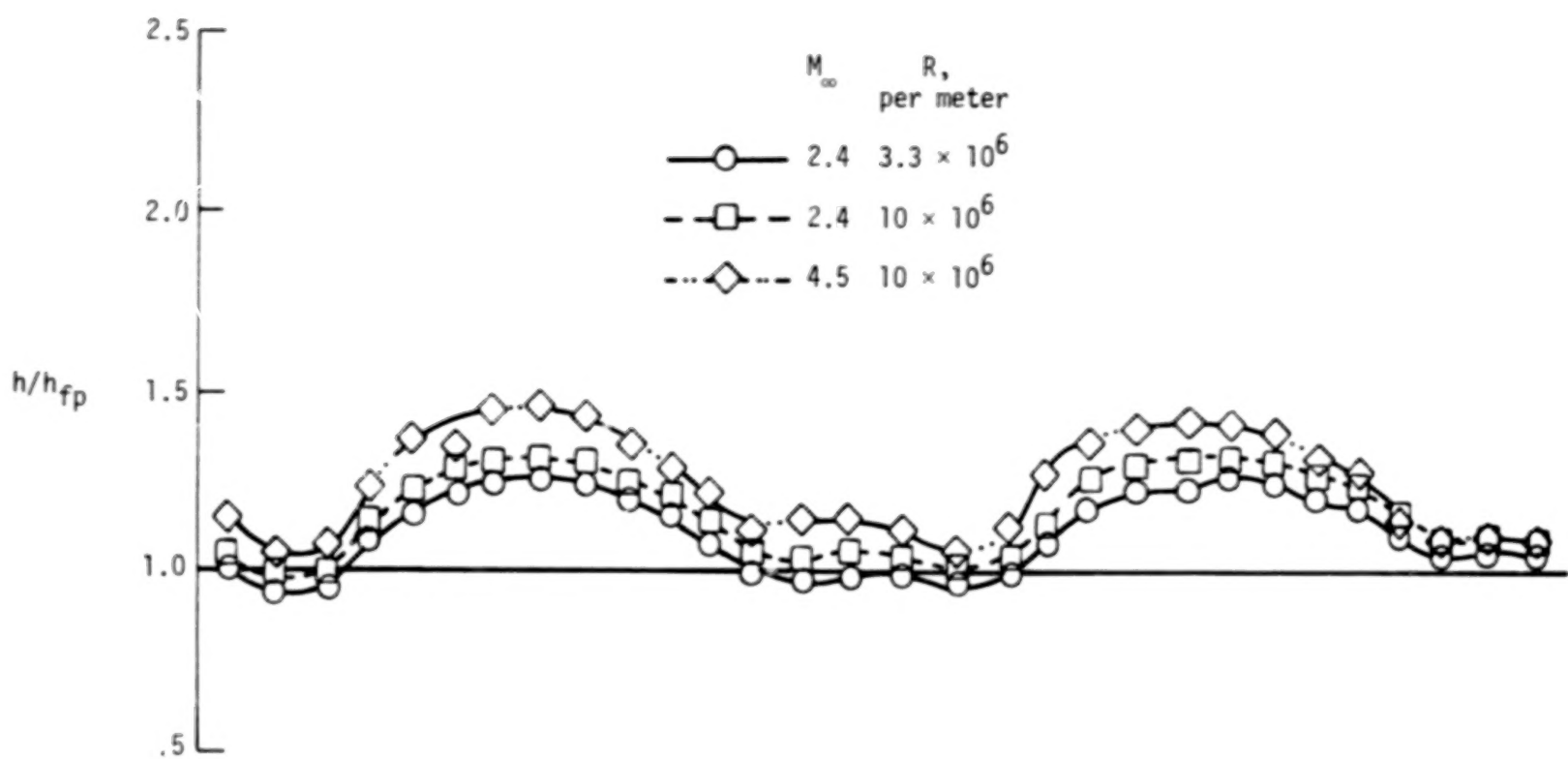
(a) $\delta = 2.5$ cm.

Figure 11.- Pressure drag coefficients for corrugated surface as a function of cross-flow angle.



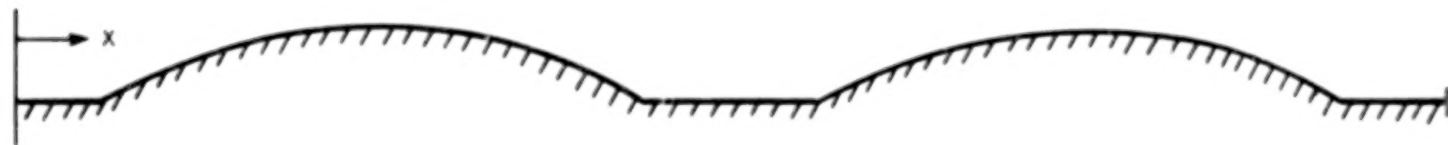
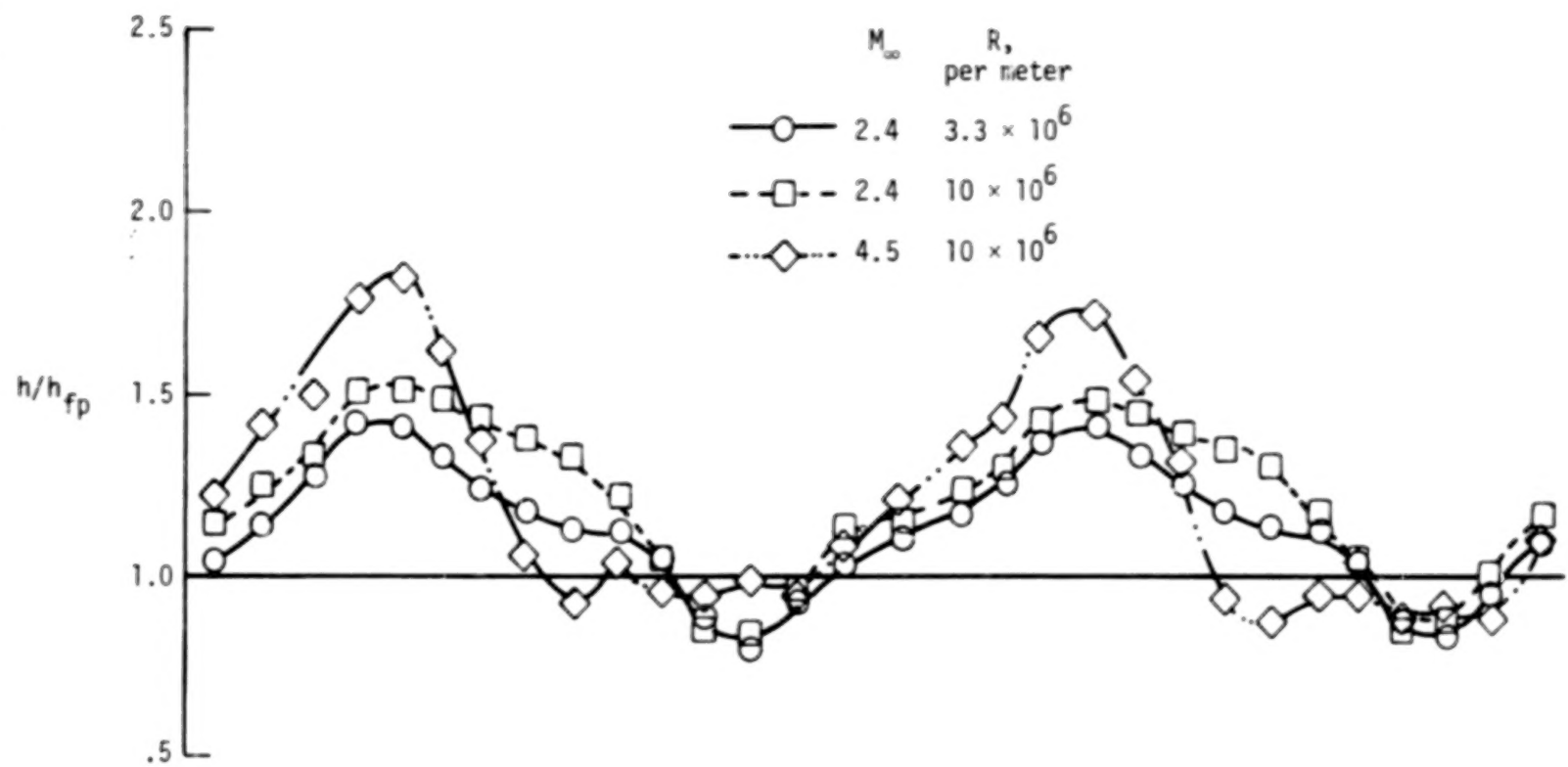
(b) $\delta = 12.7$ cm.

Figure 11.- Concluded.



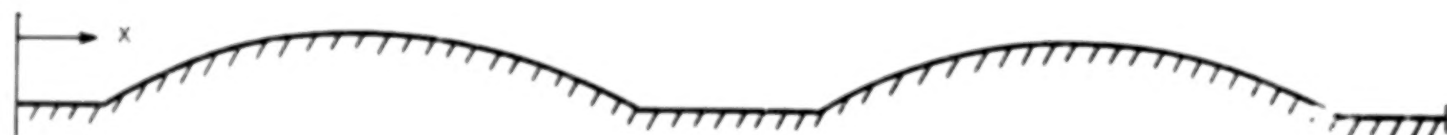
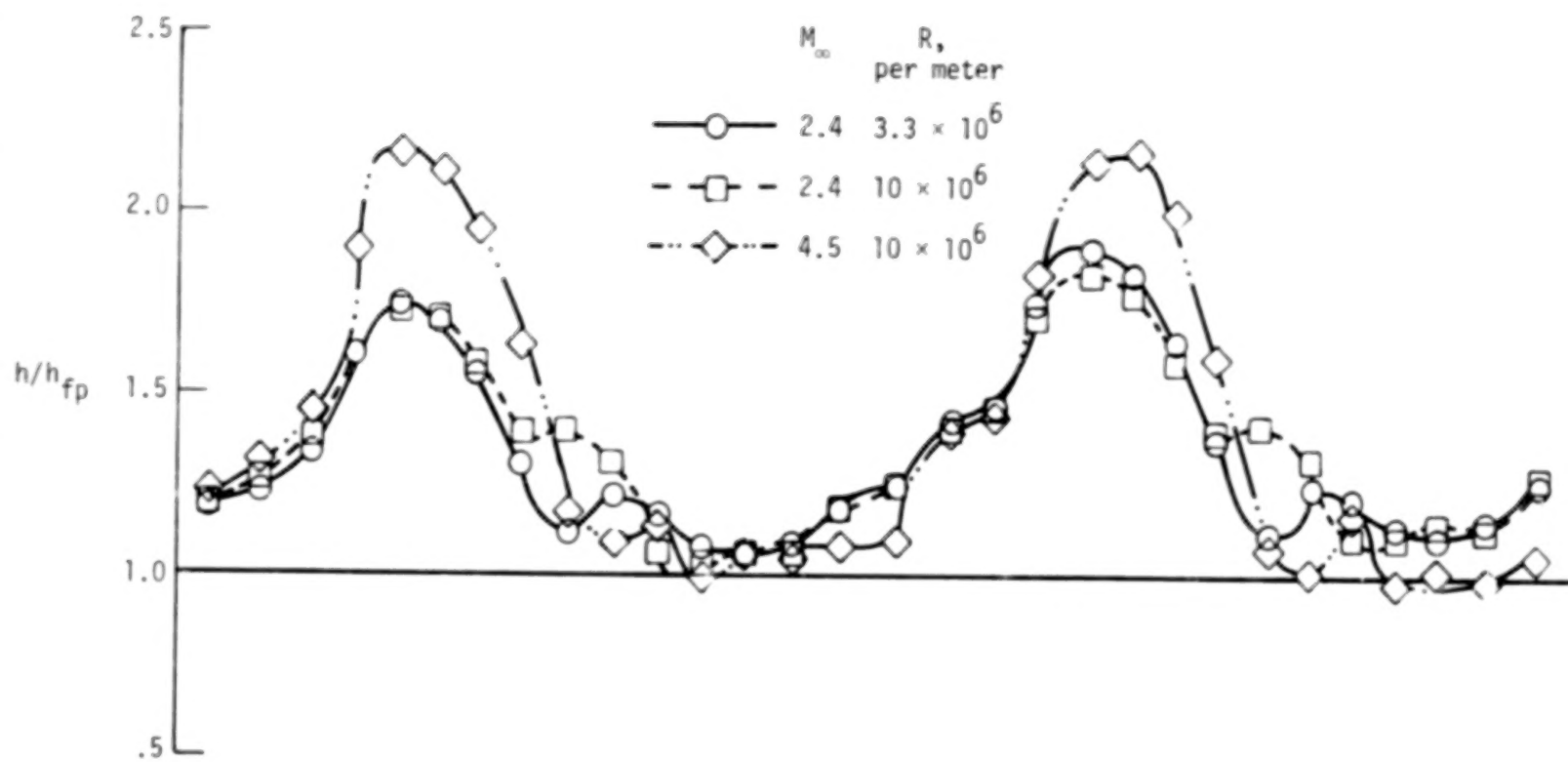
(a) $\Lambda = 0^\circ$.

Figure 12.- Heating-rate distributions over corrugated surface. $\delta = 12.7$ cm.
Table II gives thermocouple x-locations.



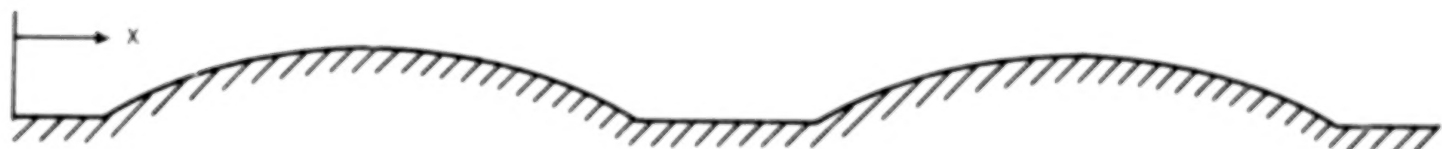
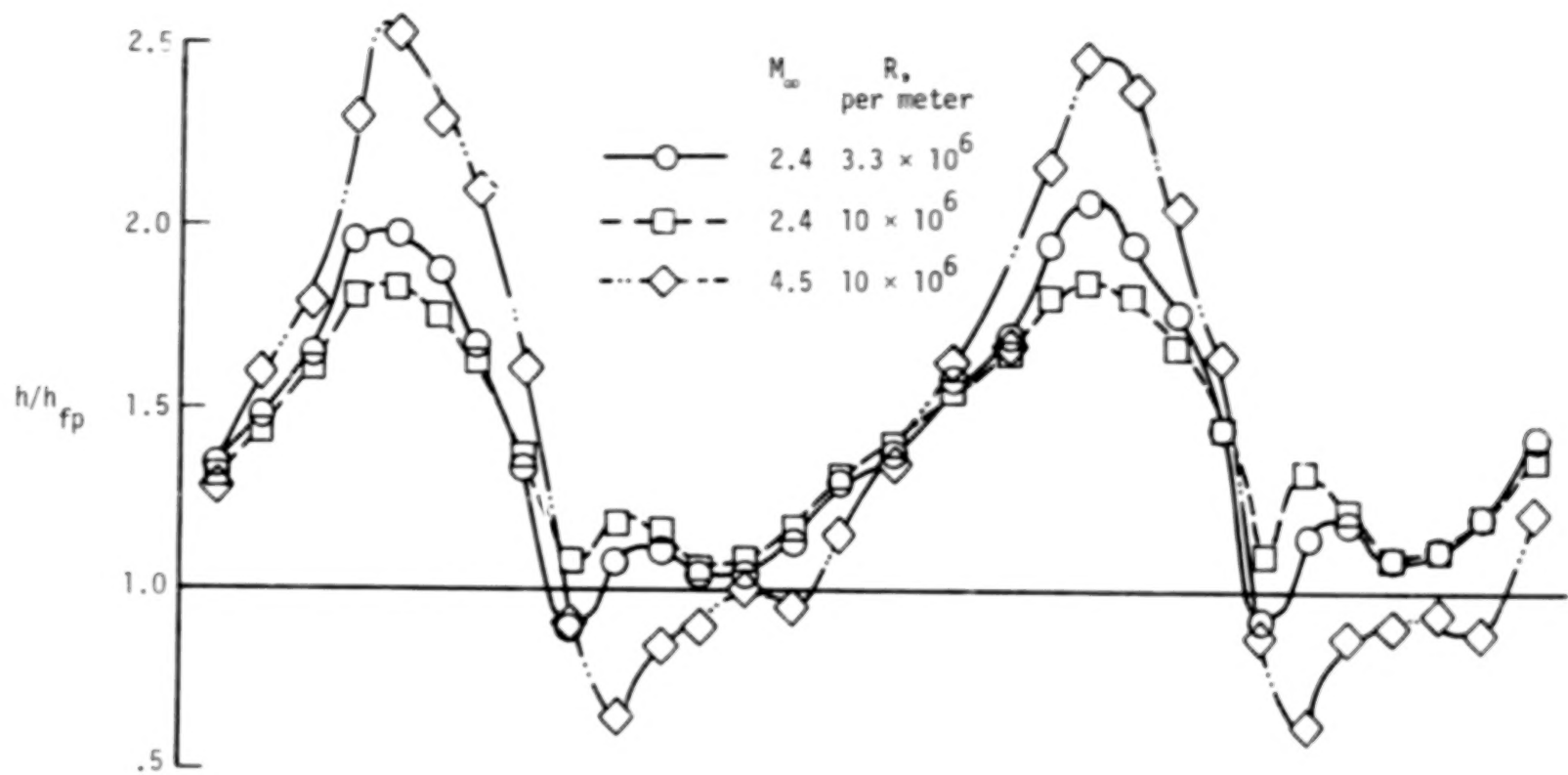
(b) $\Lambda = 15^\circ$.

Figure 12.- Continued.



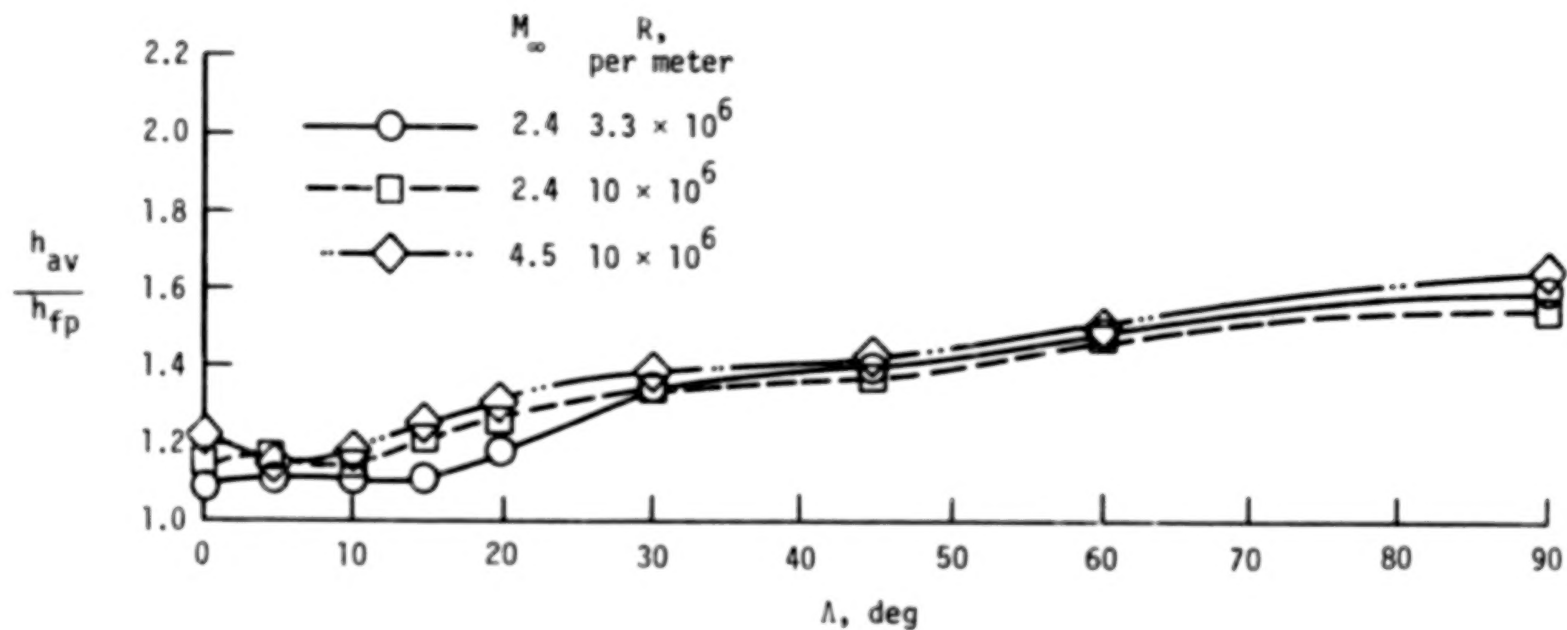
(c) $\Lambda = 30^\circ$.

Figure 12.- Continued.



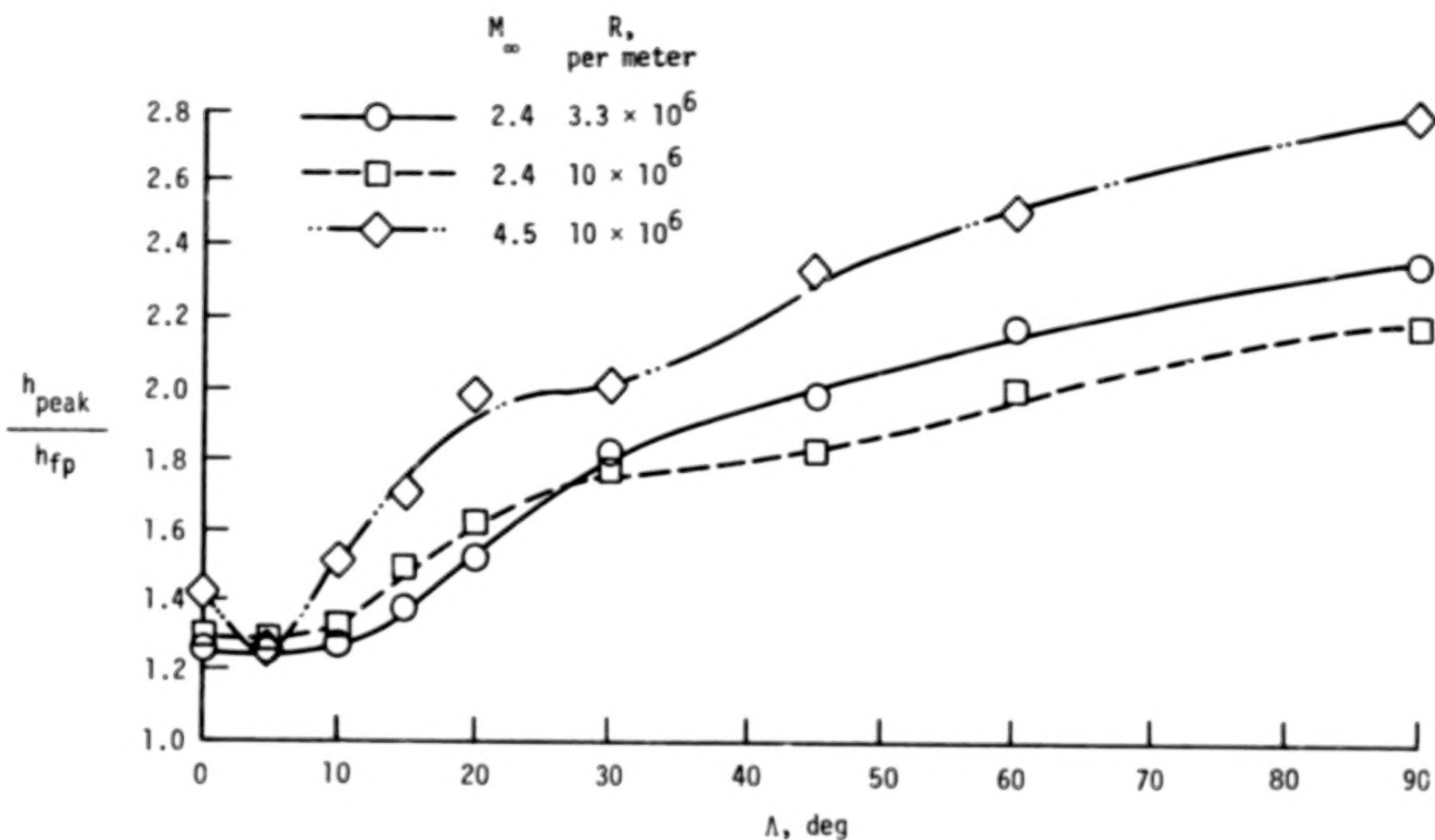
(d) $\Lambda = 45^\circ$.

Figure 12.- Concluded.



(a) Average heating rates.

Figure 13.- Average and peak heating rates for corrugated surface as a function of cross-flow angle.



(b) Peak heating rate.

Figure 13.- Concluded.

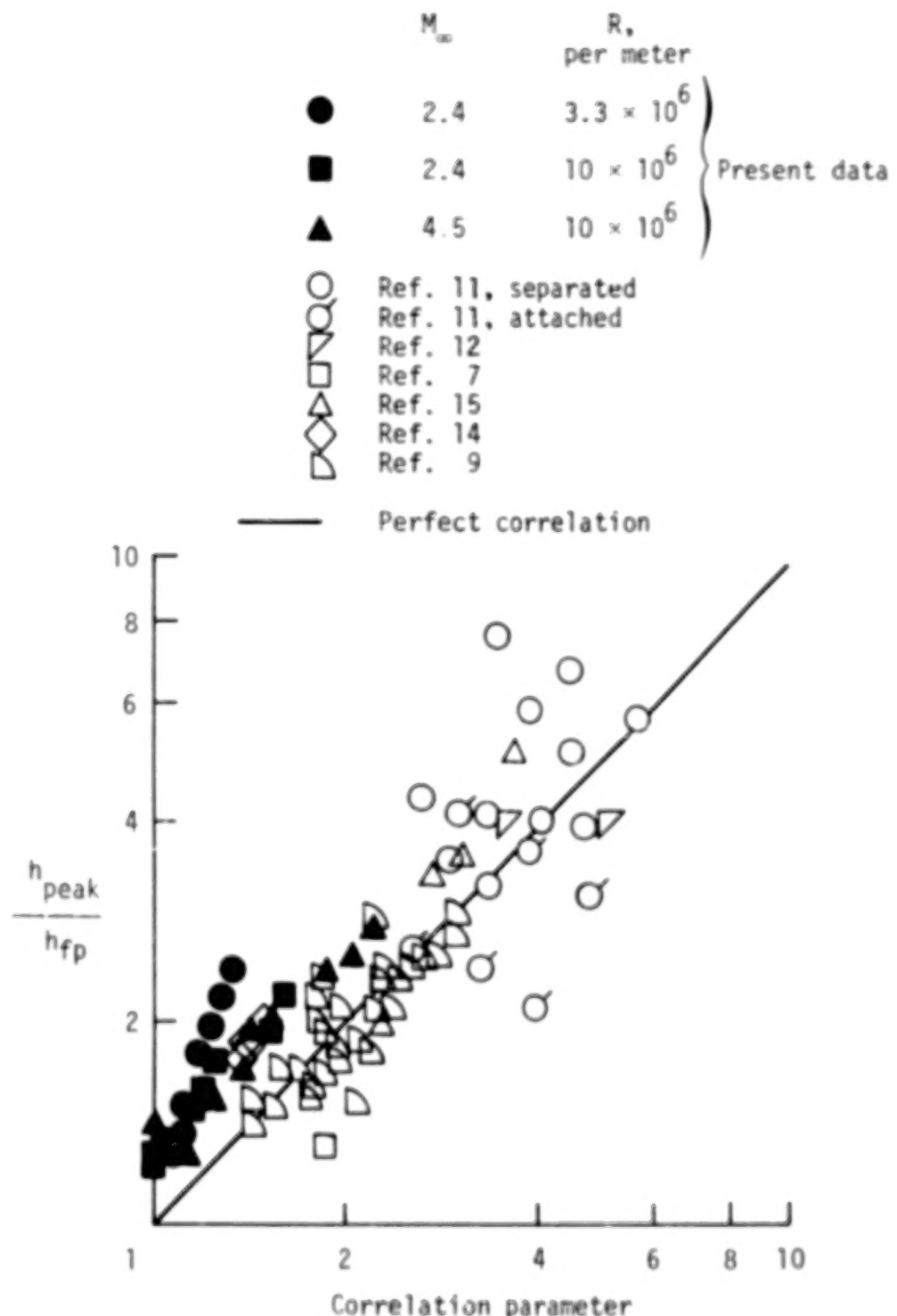
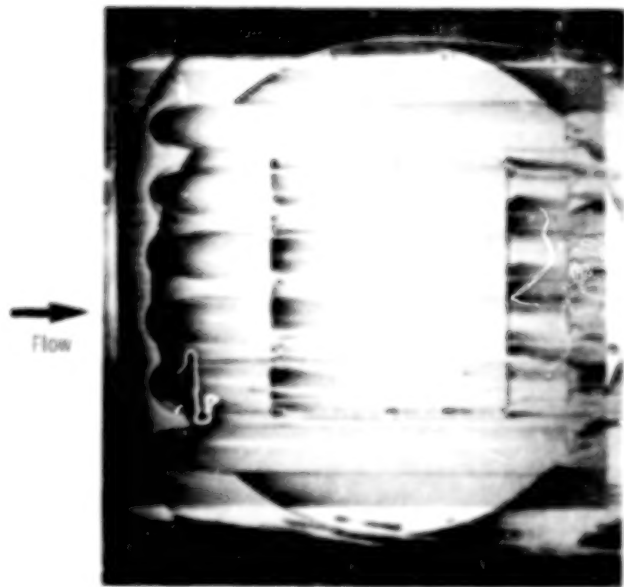
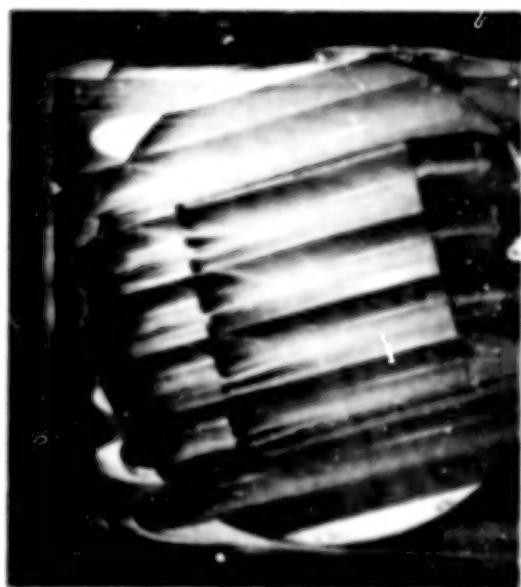


Figure 14.- Correlation of max. sum heating from present study with previously published data using parameter from reference 9. 80.



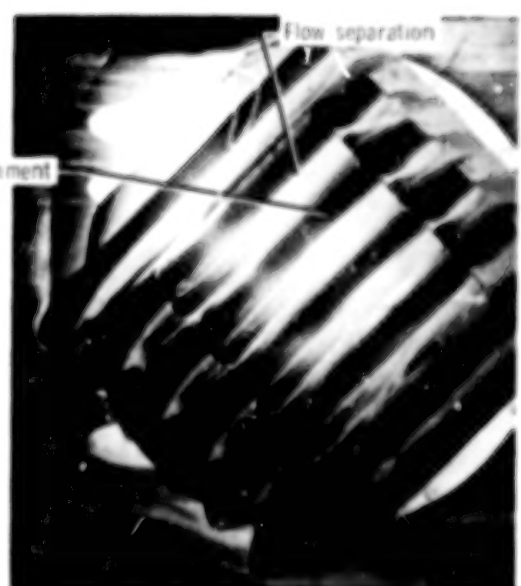
(a) $\Lambda = 0^\circ$



(b) $\Lambda = 15^\circ$



(c) $\Lambda = 30^\circ$



(d) $\Lambda = 45^\circ$

L-77-275

Figure 15.- Oil-flow patterns over corrugated surface.
 $R = 10 \times 10^6$ per meter; $\delta = 12.7$ cm.

1. Report No. NASA TP-1024	2. Government Accession No.	3. Recipient's Catalog No.		
4. Title and Subtitle PRESSURE AND HEATING-RATE DISTRIBUTIONS ON A CORRUGATED SURFACE IN A SUPERSONIC TURBULENT BOUNDARY LAYER		5. Report Date November 1977		
7. Author(s) James Wayne Sawyer		6. Performing Organization Code L-111732		
9. Performing Organization Name and Address NASA Langley Research Center Hampton, VA 23665		10. Work Unit No. 506-17-22-00		
12. Sponsoring Agency Name and Address National Aeronautics and Space Administration Washington, DC 20546		11. Contract or Grant No.		
15. Supplementary Notes		13. Type of Report and Period Covered Technical Paper		
16. Abstract <p>Drag and heating rates on wavy surfaces typical of current corrugated plate designs for thermal protection systems were determined experimentally. Pressure-distribution, heating-rate, and oil-flow tests were conducted in the Langley Unitary Plan wind tunnel at Mach numbers of 2.4 and 4.5 with the corrugated surface exposed to both thick and thin turbulent boundary layers. Tests were conducted with the corrugations at cross-flow angles from 0° to 90° to the flow. Results show that for cross-flow angles of 30° or less, the pressure drag coefficients are less than the local flat-plate skin-friction coefficients and are not significantly affected by Mach number, Reynolds number, or boundary-layer thickness over the ranges investigated. For cross-flow angles greater than 30°, the drag coefficients increase significantly with cross-flow angle and moderately with Reynolds number. Increasing the Mach number causes a significant reduction in the pressure drag. The average and peak heating penalties due to the corrugated surface are small for cross-flow angles of 10° or less but are significantly higher for the larger cross-flow angles. The measured heating rates correlated reasonably well with published results although the wave forms of the corrugations are significantly different. For cross-flow angles of 30° or greater, the flow separates from the corrugation downstream of the crest and reattaches on the upstream face of the next corrugation.</p>		14. Sponsoring Agency Code		
17. Key Words (Suggested by Author(s)) Thermal protection system Hypersonic flow Corrugated surface Metallic heat shield Aerodynamic heating		18. Distribution Statement Unclassified - Unlimited		
19. Security Classif. (of this report) Unclassified		20. Security Classif. (of this page) Unclassified	21. No. of Pages 81	22. Price ¹ \$5.00

¹ For sale by the National Technical Information Service, Springfield, Virginia 22161